small
NANO MICRO

An Overview of the Applications of Graphene-Based Materials in Supercapacitors

*Yi Huang, Jiajie Liang, and Yongsheng Chen**

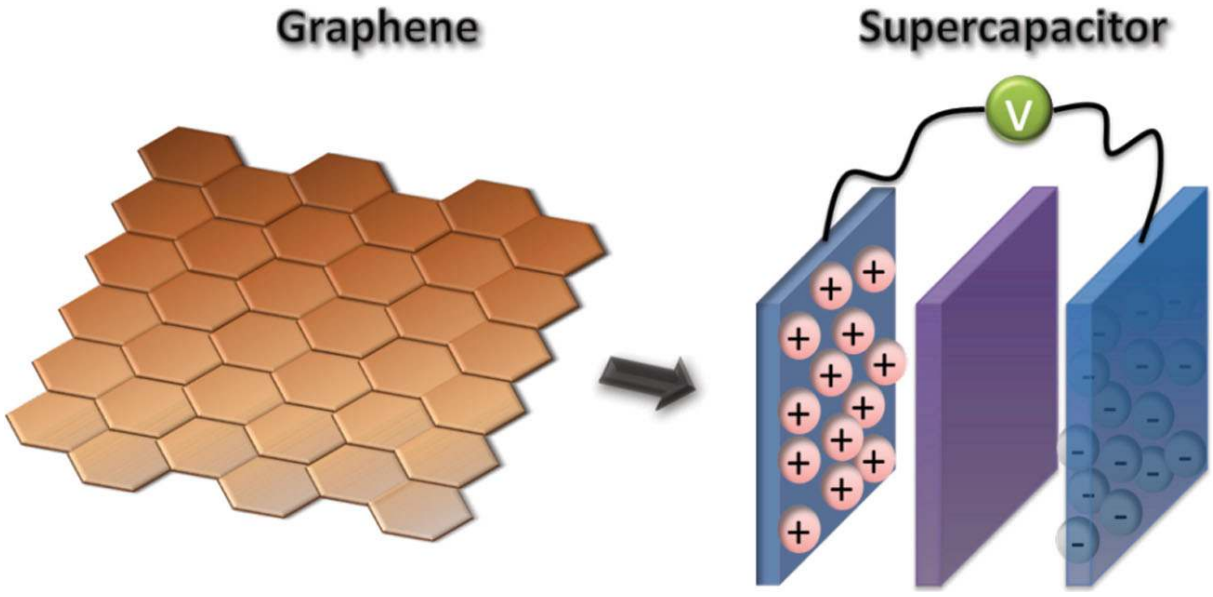

From the Contents

Due to their unique 2D structure and outstanding intrinsic physical properties, such as extraordinarily high electrical conductivity and large surface area, graphene-based materials exhibit great potential for application in supercapacitors. In this review, the progress made so far for their applications in supercapacitors is reviewed, including electrochemical double-layer capacitors, pseudo-capacitors, and asymmetric supercapacitors. Compared with traditional electrode materials, graphene-based materials show some novel characteristics and mechanisms in the process of energy storage and release. Several key issues for improving the structure of graphene-based materials and for achieving better capacitor performance, along with the current outlook for the field, are also discussed.

DOI: 10.1002/smll.201102635

1. Introduction

Graphene, a one-atom-thick 2D single layer of sp^2-bonded carbon, has been considered as the basic construction material for carbon materials of all other dimensionalities.[1–3] As a result of this unique structural property, graphene is provided with a series of prominent intrinsic chemical and physical features, such as strong mechanical strength (~1 TPa),[4,5] extraordinarily high electrical and thermal conductivity,[6–8] and large surface area (2675 m^2/g),[9] which may rival or even surpass both single- and multi-walled carbon nanotubes. These outstanding and intriguing features make this extremely versatile carbon material promising for various practical applications, including high-performance nanocomposites,[10–12] transparent conducting films,[6,7,13–16] sensors,[17,18] actuators,[19–22] nanoelectronics,[23,24] and energy storage devices.[25–28] Significantly, utilizing graphene as a supercapacitor electrode material has become the focus of a considerable amount of research in the field of clean energy devices due to the beneficial combination of the excellent mechanical and electrical properties and large surface area.[25–28]

The investigation of novel, low-cost, environmentally friendly, and high-performance energy storage systems has been under an ever increasing demand as a result of the needs of modern society and emerging ecological concerns.[29] Supercapacitors, also named electrochemical capacitors and ultracapacitors,[30,31] are supposed to be a promising candidate for alternative energy storage devices as a result of their high rate capability, pulse power supply, long cycle life, simple principles, high dynamic sof charge propagation, and low maintenance cost.[31–34] Supercapacitors store significantly higher amounts of energy density than the conventional dielectric capacitor, but they have a similar cell construction as traditional capacitors except for the fact that the metal electrodes are replaced by highly porous electrodes.[35] Furthermore, the shortage of other power sources, such as batteries and fuel cells, could be complemented by supercapacitors, because of their long cycle life and rapid charging and discharging rate at high power densities.[34] Consequently, the supercapacitor has continued to attract considerable attention from both scientists and engineers since it was demonstrated and patented by General Electric[36] in 1957, and it has generated great interest for a wide and growing range of applications that require high power density such as energy back-up systems, consumer portable devices, and electrical/hybrid automobiles.[33,34,36–38]

Actually, based on the different energy storage mechanisms, supercapacitors can be divided into two classes: 1) electrochemical double-layer capacitors (EDLCs) which store energy using the adsorption of both anions and cations and 2) pseudo-capacitors that store energy through fast surface redox reactions. EDLCs, which are non-Faradaic ultracapacitors, derive their performance from a so-called double-layer capacitance.[39,40] The capacitance in these EDLC devices is stored as a build-up of charge in the layers of the electrical double-layer formed at the interface between a high-surface-area electrode and an electrolyte.[39,40] Generally, porous carbon materials such as activated carbon,[41,20] xerogels,[43] carbon nanotubes (CNTs),[44–47] mesoporous carbon,[48] and carbide-derived carbons,[49] have been investigated for use as electrodes in EDLCs. Extensive explorations have shown that to achieve EDLCs with high performance, several factors of the carbon-based materials are crucial: the specific surface area (SSA), electrical conductivity, and pore size and distribution. In most cases, although porous-carbon-based materials can obtain high SSA, the low conductivity of porous carbon materials continues to restrict its application in high-power-density supercapacitors.[50] As for CNTs, although they possess high electrical conductivity and large SSA, CNT-based supercapacitors still cannot meet acceptable performance,[44,51–53] which is probably due to the observed contact resistance between the electrode and current collector.[48,50] Moreover, the intrinsic impurities of CNTs from catalysts and amorphous carbon and their high cost have hampered their practical application in supercapacitors to date. Hence, great efforts are still spent on developing novel carbon-based supercapacitor electrode materials with an overall high performance. Fortunately, the emergence of graphene provides an excellent alternative to past EDLC electrode materials. Compared with traditional porous carbon materials, graphene has very high electrical conductivity, large surface area, and profuse interlayer structure. Hence graphene-based materials are hugely favorable for their application to EDLCs.[27]

In contrast to EDLCs, pseudo-capacitors store energy through a Faradic process, involving fast and reversible redox reactions between electrolyte and electro-active materials on the electrode surface.[40] The most widely explored electro-active materials include three types: a) transition metal oxides or hydroxides,[54,55] such as ruthenium oxide, manganese oxide, and nickel hydroxide; b) conducting polymers,[39,41,56] such as polyaniline, polypyrrole, and polythiophene; and c) materials possessing oxygen- and nitrogen-containing surface functional groups.[40] Compared with EDLCs, pseudo-capacitors can achieve much higher pseudo-capacitance than the EDL capacitance. Nevertheless, further practical applications of these electro-active materials to pseudo-capacitors are still limited by the low power density that arises from the poor electrical conductivity restricting fast electron transport, and by the lack of a pure cycling stability owing to the easily damaged structure of the materials during the redox process. Hence, to resolve these problems, carbon-based materials with high electrical conductivity and large SSA are usually used as the backbone materials to combine with these active materials for pseudo-capacitor electrodes. Given the many excellent properties of graphene, such as high electrical conductivity and high mechanical strength, graphene is

Prof. Y. Huang,[+] Dr. J. J. Liang,[+] Prof. Y. S. Chen
Key Laboratory of Functional Polymer Materials
and Centre for Nanoscale Science and Technology
Institute of Polymer Chemistry
College of Chemistry
Nankai University
300071, Tianjin, China
E-mail: yschen99@nankai.edu.cn
[+] Y. L. and J.J.L. have contributed equally to this review.

DOI: 10.1002/smll.201102635

small NANO MICRO

considered as one of the most suitable substrate materials for preparing pseudo-capacitor electrodes.

In this review, we will summarize the progress made so far in graphene-based supercapacitors by considering to the two basic kinds of supercapacitors (EDLCs and pseudo-capacitors) and their hybrid supercapacitors (which function with simultaneous EDLC and pseudo-capacitor mechanisms); we will discuss their mechanisms and explore their effective ways to achieve high supercapacitor performance.

2. Preparation of Graphene-Based Materials used for Supercapacitor Electrodes

Several effective and facile approaches have been developed to synthesize graphene-based materials, including: 1) epitaxial growth and chemical vapor deposition (CVD) growth of graphene on SiC and matched metal surfaces;[14,57–59] 2) micromechanical exfoliation of graphite (using atomic force microscopy (AFM) cantilevers or adhesive tape);[5,7,60] 3) exfoliation of graphite in organic solvents;[61] 4) substrate-free gas-phase synthesis of graphene platelets in a microwave plasma reactor;[62] 5) arc-discharge synthesis of multi-layered graphene;[63] 6) reduction from graphene oxide (GO), which is synthesized by either the Brodie,[64] Staudenmaier,[65] or Hummers methods,[66] and variations of these chemical exfoliation methods. Although the number of different fabrication methods continually increases,[58] the most important method to prepare graphene-based materials that can be used for supercapacitor electrodes is still the chemical exfoliation of graphite to graphene oxide, followed by controllable reduction of graphene oxide to graphene.[11,13,67] This is probably attributed to the following reasons: 1) graphene oxide can be facilely prepared through the chemical exfoliation method at large-scale with relatively low cost, which is the first condition required for the practical application of graphene-based supercapacitors. 2) The oxygen-containing functional groups on the surface allow for graphene oxide to be easily chemically modified and processed in solution state. 3) Various routes can be used to reduce GO to graphene, restore the intrinsic SSA and electrical conductivity of graphene, and construct graphene-based nanostructures with desirable channel size, which are all favorable for supercapacitor applications. Thus, as we will discuss in the following sections, exploring novel ways to reduce GO to graphene and to design graphene-based materials with high SSA and conductivity are the main-stream routes, but these are not the only way to construct high-performance graphene-based supercapacitor electrodes.

3. Graphene-Based EDLCs:

3.1. Graphene-Based Electrode Materials Prepared through Chemical Reduction of Graphene Oxide

Suspending graphene oxide sheets in water followed by reducing them (with reducing agent such as hydrazine hydrate) is a simple yet versatile method to prepare reduced graphene-based materials (RGM).[68] Ruoff and co-workers[38] first explored graphene-based EDLCs utilizing this kind of chemically modified graphene (CMG) as electrode materials. Although the individual graphene sheets partially agglomerated into particles approximately 15–25 μm in diameter during the reduction process, the relatively high specific surface area of the graphene-based material (GBM) aggregation (705 m^2/g) still allows these CMG electrodes to have high electrochemical performance (**Figure 1**). Large specific capacitance values of 135 and 99 F/g for aqueous and organic electrolytes, respectively, were achieved by these CMG materials. Moreover, low variation of specific capacitance for increasing voltage scan rates was also observed for the CMG electrodes due to the high conductivity of the CMG (~200 S/m). Given that there is still much potential for the improvement of the SSA and conductivity of graphene-based

Yongsheng Chen graduated from the University of Victoria with a Ph.D. degree in chemistry in 1997 and then joined the University of Kentucky and the University of California at Los Angeles for postdoctoral studies from 1997 to 1999. From 2003, he has been a Chair Professor at Nankai University. His main research interests include: 1) carbon-based nanomaterials, including carbon nanotubes and graphene; 2) organic and polymeric functional materials, and 3) energy devices including organic photovoltaics and supercapacitor. He has published over 130 peer-reviewed papers with over 6000 citations and has over 20 patents.

Yi Huang received his B.S. (1996) in Polymer Science and Engineering and Ph.D. (2001) in Materialogy from Sichuan University. He then spent two years as a postdoctoral fellow at the Department of Chemical Engineering of Tsinghua University. Since 2004, he has been an Associate Professor of Chemistry at Nankai University. His research interests focus on controlled synthesis and application of carbon nanomaterials (graphene and carbon nanotubes), functional polymer materials, and nano-composites and -devices. He has published over 60 peer-reviewed journal articles with over 1500 citations.

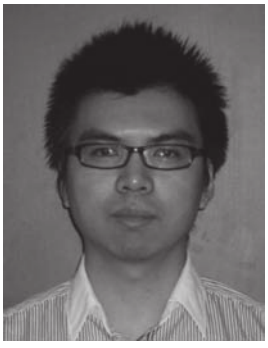

Jiajie Liang received his B.S. from the Department of Chemistry of Nankai University (2006) and his Ph.D. from the Institute of Polymer Chemistry of Nankai University under the direction of Prof. Yongsheng Chen (2011). Currently, he is a postdoctoral fellow in the group of Prof. Qibing Pei in the Department of Materials Science & Engineering at the University of California, Los Angeles. His research is focused on the applications of graphene-based materials, including graphene-based actuators, high-performance composites, and electronic devices.

DOI: 10.1002/smll.201102635

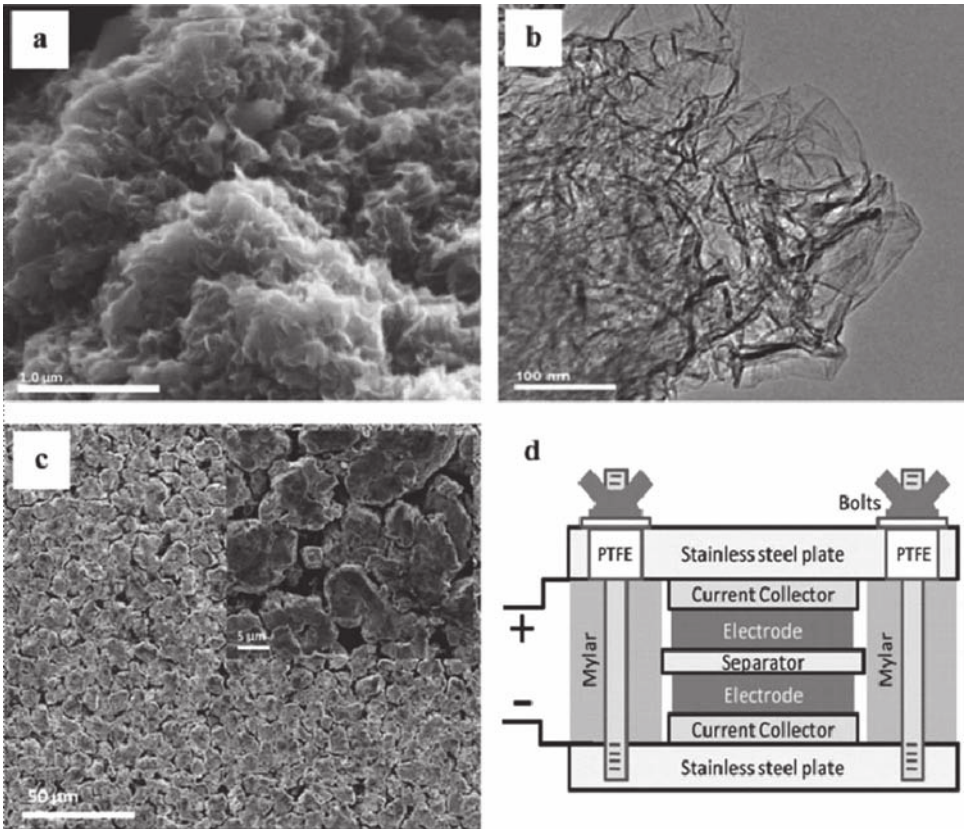

Figure 1. Graphene-based EDLCs utilizing CMG as electrode materials. a) Scanning electron microscopy (SEM) image of CMG particle, b) transmission electron microscopy (TEM) image showing individual graphene sheets extending from the CMG particle, c) low- and high- (inset) magnification SEM images of the CMG particle electrode, and d) schematic of test cell assembly. Reproduced with permission.[38] Copyright 2008, American Chemical Society.

materials, this original work and encouraging results indicate that graphene-based materials are extremely promising candidates for EDLC ultracapacitors.

Although GO can be well dispersed in aqueous solution as individual sheets, direct reduction of GO in solution will result in irreversibly precipitated agglomerates,[68] which behave no differently than particulate graphite platelets having relatively low surface area.[69] To avoid this irreversible re-stacking of graphene, Chen and co-workers[70] exploited a gas–solid reduction process to prepare the graphene-based materials, and fabricated supercapacitor devices using these GBM as electrode materials. While the graphene sheets still exist as aggregated and crumpled sheets closely associated with each other and form a continuous conducting network, this GBM indeed has a low degree of agglomeration (**Figure 2**) compared with the graphene material obtained in a solution reduction process.[38,68] Thus, in this structure or morphology, the electrolyte ion should have better accessibility, not only penetrated in the outer region of the solids but also in the inner region compared with conventional carbon materials used in capacitors. Consequently, both ends of a broad range of graphene sheets could be exposed to the electrolyte and thus contribute to the capacitance. As a result, a maximum specific capacitance of 205 F/g with a measured power density of 10 kW/kg at an energy density of 28.5 W h/kg in an aqueous electrolyte solution has been achieved by this GBM electrode. In addition, the supercapacitor devices exhibit excellent long cycle life along with ~90% specific capacitance retained after 1200 cycle tests.

In addition to hydrazine hydrate, hydrobromic acid is another widely used agent that can reduce GO. Ma and co-workers[71] reported that adding hydrobromic acid into a GO solution reduces it to graphene-based materials. Since hydrobromic acid is a weak reductant, some oxygen functional groups, which are relatively stable for electrochemical systems, remain in reduced GO. Therefore, the oxygen-containing groups on the graphene surface not only can promote the wettability of the reduced GO and facilitate the penetration of the aqueous electrolyte, but they also introduce pseudo-capacitive effects. As a result, at the current density of 0.2 A/g, the maximum specific capacitance values reach 348 F/g in the 1 M aqueous H_2SO_4. Surprisingly, the capacitance of reduced GO does not degrade but increase continuously until the 2000th cycle. More specifically, it passes 125% of the initial capacitance after 1800 cycles and is still above 120% after 3000 cycles. These may be due to the fact that the reduction of the residual oxygen by the cycling measurements continuously improves the capacitive properties before the 1800th cycle.

small 2012,
DOI: 10.1002/smll.201102635

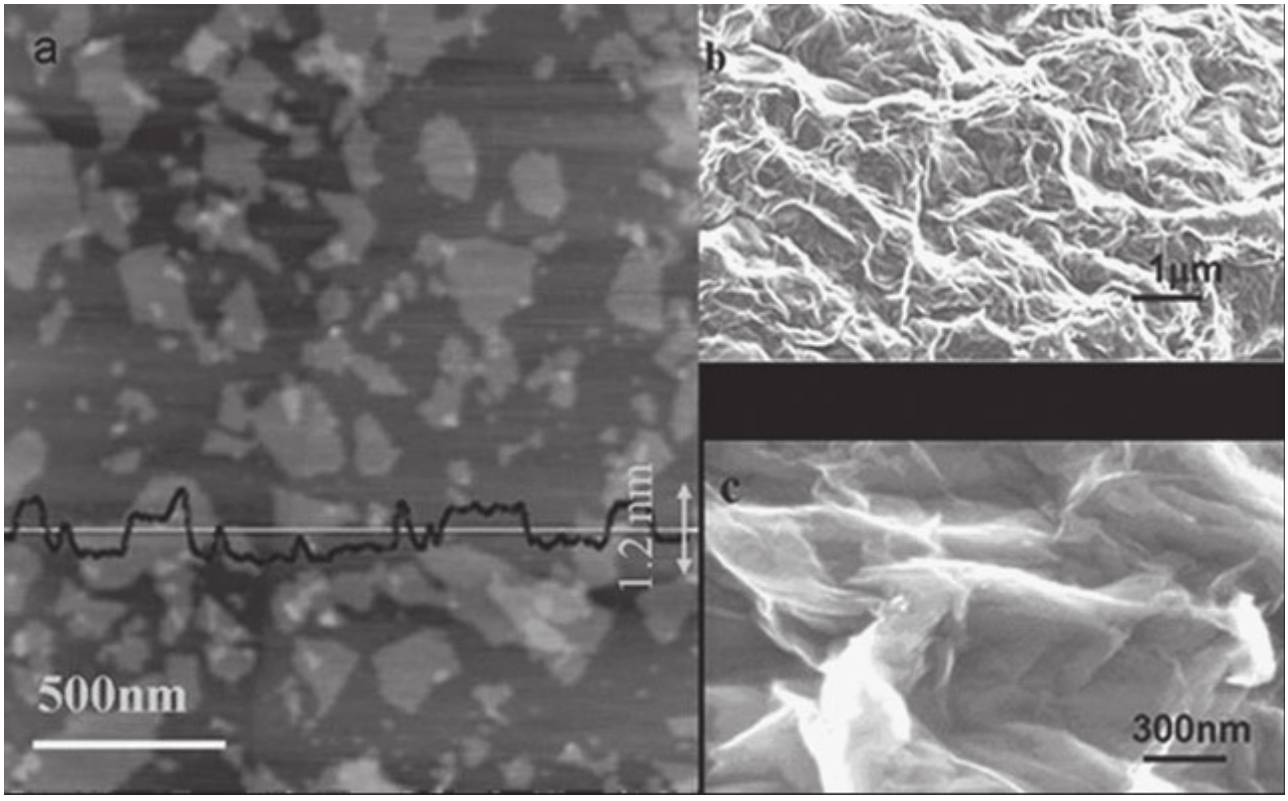

Figure 2. Morphology of graphene oxide and graphene-based materials as prepared by Chen and co-workers. a) Tapping-mode AFM image of graphene oxide and height profile plot. b,c) SEM images with different scale bars. Reproduced with permission.[70] Copyright 2009, American Chemical Society.

3.2. Graphene-Based Electrode Materials Prepared through Thermal Reduction of Graphene Oxide

RGM can also be prepared via thermal exfoliation of GO. It has been reported that GO can be exfoliated into RGM when the temperature is higher than 550 °C at normal pressure.[72–74] Accordingly, RGM prepared through exfoliation at 1050 °C have been investigated as electrode materials in EDLCs by Rao and co-workers.[35] These samples, which are provided with SSA values as large as 925 m^2/g, exhibit specific capacitance values reaching up to 117 F/g in aqueous H_2SO_4 electrolyte.

However, this high-temperature exfoliation process is energy-consuming and difficult to control; therefore, a relatively low-temperature exfoliation method was developed. While carried out under a high-vacuum environment, Yang and co-workers[75] reported that the GO exfoliation process can be conducted at temperatures as low as about 200 °C. It is proposed that the graphene sheets in these low-temperature exfoliation samples tend to overlay each other forming an aggregated structure with large pores, through which the electrolyte ions can easily access the surface of graphene to form electric double layers (**Figure 3**). Benefiting from this open core system and the unique surface chemistry due to the low-temperature exfoliation, the capacitances of these few-layered graphene-based electrodes for aqueous and organic systems are 264 and 122 F/g, respectively, for the tenth cycle at a current density of 100 mA/g; these values are much higher than those of high-temperature exfoliation samples.[35] In another report, Cao and co-workers[76] prepared RGM using GO as the precursor via a low-temperature thermal exfoliation approach in air. The obtained samples possessed large specific capacitance values, reaching 232 F/g at a current density up to 1 A/g in 2 M KOH. Given the moderate Brunauer–Emmett–Teller (BET) specific surface area for this graphene-based material, such a high specific capacitance value is considered to originate from the electrochemical double-layer capacitance from the graphene sheets and the pseudo-capacitance from the oxygen-containing groups existing on the surface of the graphene sheets. However, these functional groups may have a negative effect on the stability of the EDL capacitance.

A mild solvothermal method was also employed to reduce GO to fabricate RGM supercapacitor electrodes. This is a relatively low-temperature exfoliation and reduction method that can be used to reduce the individual GO platelets dispersed in a suitable solvent without using reducing agents. Ruoff and co-workers[77] found that GO can be exfoliated and well dispersed in propylene carbonate (PC) solvent via sonication treatment; furthermore, thermally heating the suspension to 150 °C can remove a significant fraction of the oxygen functional groups on the GO, and the reduced sample, which is composed of a stack of reduced graphene platelets with the number of layers ranging from 2 to more than 10,

DOI: 10.1002/smll.201102635

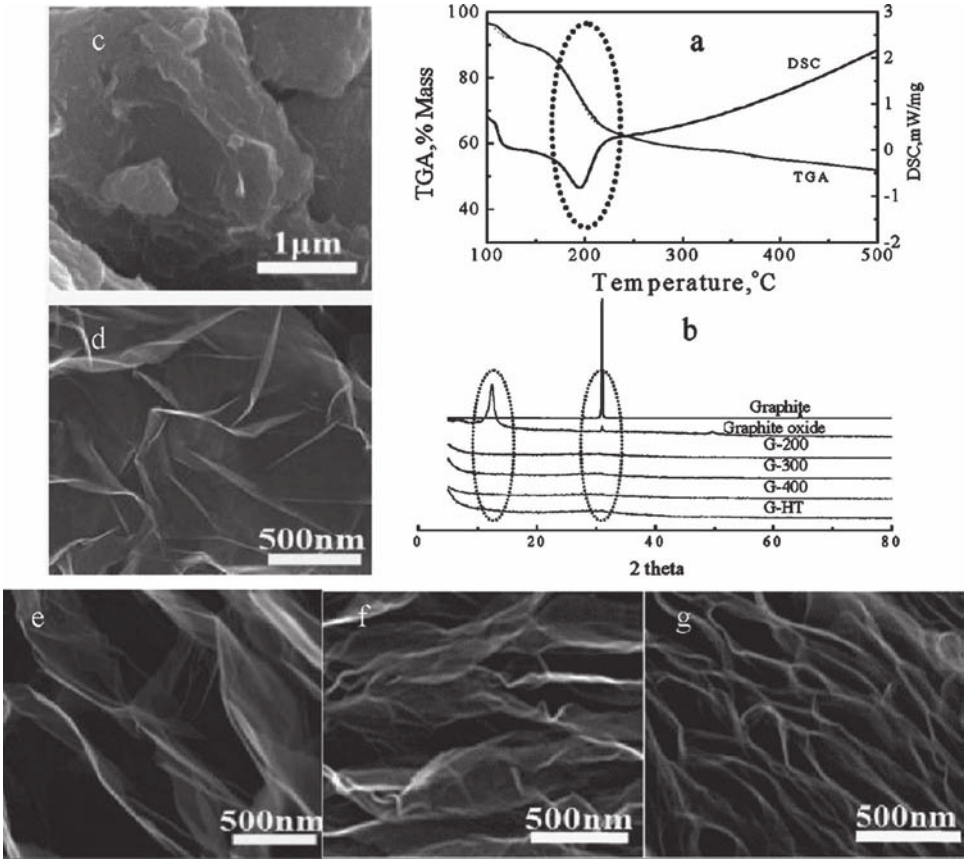

Figure 3. Structural characterization of a graphite oxide and graphene. a) Thermogravimetric and differential scanning calorimetry (TG-DSC) curves of a GO sample. b) X-ray diffraction (XRD) patterns of graphite, GO, and the graphene resulting from exfoliation. c–g) SEM images of G-200, G-400, G-200-HT, and G-HT (G-200, G-300, and G-400 correspond to the thermally treated samples at 200, 300,and 400 °C respectively; G-200-HT corresponds to heat-treating G-200 in a preheated furnace at 1000 °C; G-HT corresponds to a sample prepared by a normally employed high-temperature exfoliation method at 1000 °C). Reproduced with permission.[75] Copyright 2009, American Chemical Society.

in PC remains a homogeneous black suspension. Although reduced under relatively low temperature, such reduced graphene platelets still showed a conductivity value as high as 5230 S/m. Since commercial ultracapacitors commonly use tetraethylammonium tetrafluoroborate (TEA BF_4) in PC for the electrolyte, TEA BF_4 could be simply added to this PC/RGM suspension with the resulting slurry then used for the EDLC electrodes. A high capacitance of 112 F/g was achieved by this RGM in a PC-based electrolyte, which compares favorably with the performance of other electrode materials (80–120 F/g) using PC-based electrolytes.[78] In another work, Wong and co-workers[79] dispersed GO in dimethyl formamide (DMF) and thermally treated the dispersion at a moderate temperature (150 °C), which allows fine control of the density of functional groups. Importantly, such surface functionalities on graphene introduce high pseudo-capacitance, good wetting properties, and acceptable electrical conductivity to these graphene-based materials. They found that the specific capacitance between 0 and 0.5 V is much larger than that between 0.6 and 0.8 V. These results together with cyclic voltammetry (CV) curves suggests that EDLC is responsible for the capacitance between 0.6 and 0.8 V and pseudo-capacitance becomes the dominant contributor at lower potentials (**Figure 4**). A specific capacitance up to 276 F/g was gained based on functionalized graphene at a discharge current of 0.1 A/g in a 1 M H_2SO_4 electrolyte. Surprisingly, although the surface functional groups provide high pseudo-capacitance due to the redox reactions, the graphene-based materials still show good cycling stability. The reason behind this is that the pseudo-capacitance mainy arose from the the dominating fraction of carbonyl and hydroxyl groups on the graphene surface, but not the carboxyl groups which sometimes lead to degradation of carbon materials.[80,81] The carboxyl groups can be efficiently removed, but the carbonyl and hydroxyl groups can be retained due to their high thermal stability during the solvothermal reaction; a high pseudo-capacitance is thus obtained without sacrificing the cycling stability.

As a convenient and rapid heating source, microwave irradiation annealing has also been used to prepare exfoliated graphite (EG) from a wide range of graphite intercalation compounds (GICs) due to the microwave absorbing properties of graphene-based materials.[82–86] On the basis of this technique, Ruoff and co-workers[82] prepared RGM by facilely and efficiently treating GO powder in a commercial microwave oven. This as-prepared sample consisted of crumpled, "worm-like", few-layer thick (**Figure 5**), and

DOI: 10.1002/smll.201102635

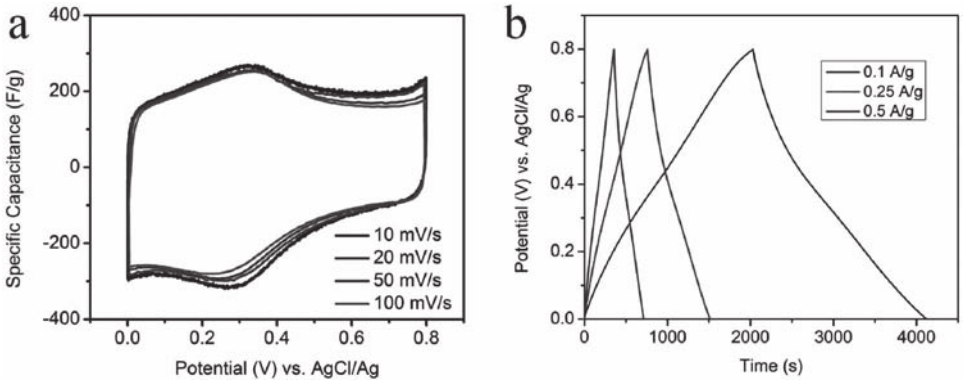

Figure 4. Capacitive properties of functionalized graphene materials (fG). a) CV curves of fG at different scan rates; b) galvanostatic charge/discharge curves of fG at different charge/discharge currents. 1 M H_2SO_4 was used as electrolyte. Reproduced with permission.[79] Copyright 2011, American Chemical Society.

electronically conductive graphitic sheets. They showed a specific surface area of 463 m^2/g, which make it a promising electrode material for EDLC applications. Therefore, employing the microwave-exfoliated RGM as an electrode material in an EDLC, specific capacitance values as high as 191 F/g were obtained with KOH electrolyte. This simple microwave irradiation annealing process provides a promising route for the scalable and cost-effective production of graphene-based electrode materials.

3.3. Graphene-Based Electrode Materials Prepared through Graphene-Based Hydrogel

In most cases, graphene-based electrodes prepared simply through chemical and/or thermal reduction still do not have sufficiently large pores for the facile access of the electrolyte.[8,36,87–89] As a result, the high specific capacitances and energy densities were in most studies only achievable by charging/discharging at low current densities (<1 A/g) or

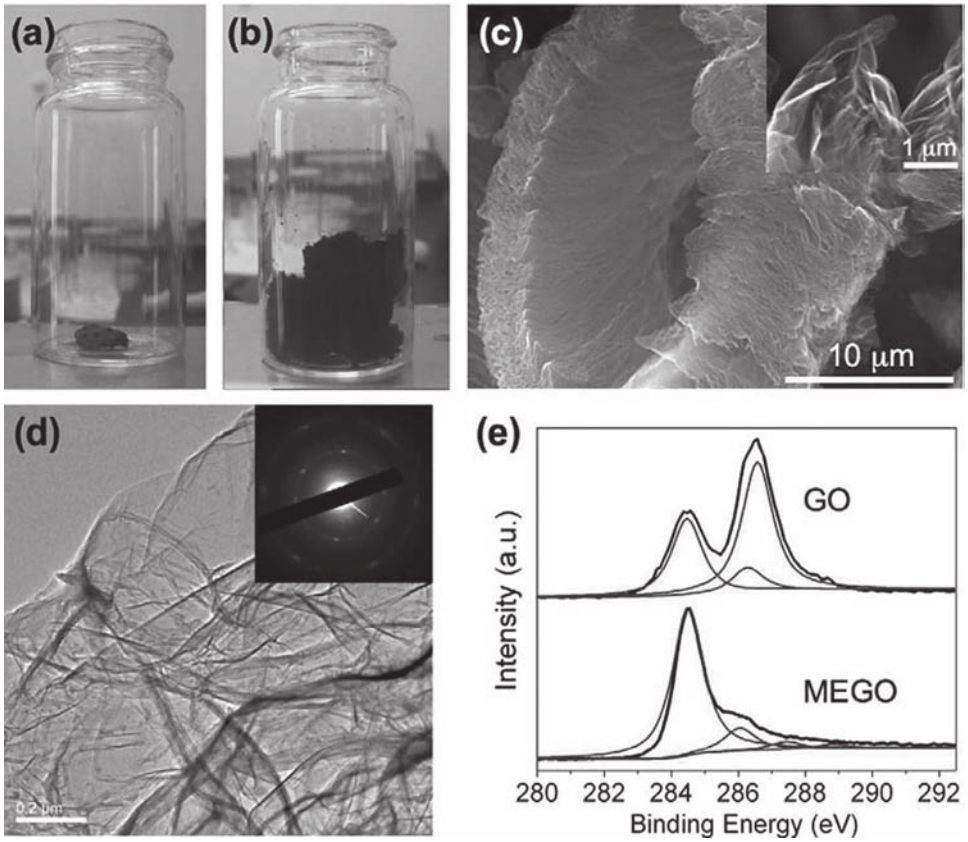

Figure 5. Structure characterization of GO. Optical photos of GO before (a) and after (b) treatment in a microwave oven for 1 min. c) SEM image of as-prepared microwave-exfoliated GO by microwave irradiation with a high-magnification SEM image in the inset. d) TEM image of the microwave-exfoliated GO with electron diffraction pattern. e) X-ray photoelectron spectroscopy (XPS) C 1s spectra of GO and microwave-exfoliated GO (MEGO). Reproduced with permission.[82] Copyright 2010, Elsevier Ltd.

DOI: 10.1002/smll.201102635

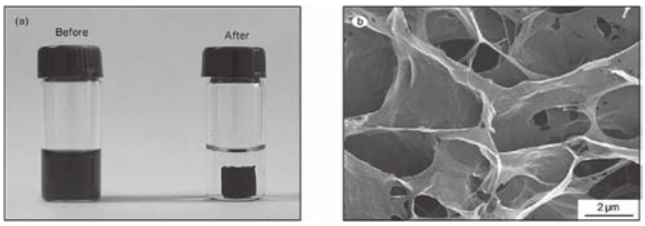

Figure 6. a) Photograph of an aqueous mixture of GO (2 mg/mL) and sodium ascorbate before (left) and after (right) chemical reduction. b) SEM image of AQSGH. Reproduced with permission.[87] Copyright 2010, American Chemical Society.

cyclic voltammetry scanning at low potential scan rates (<50 mV/s). Less-agglomerated, self-supported, and binder-free graphene-based electrodes with suitable pore sizes are still highly needed. Recently, a novel kind of 3D self-assembled graphene hydrogel prepared by chemical reduction of the aqueous GO dispersion with sodium ascorbate has been reported by Shi's group.[87] As shown in **Figure 6**, this graphene hydrogel has a well-defined and cross-linked 3D porous structure with pore sizes in the range of sub-micrometers to several micrometers. Furthermore, the graphene hydrogels are electrically conductive (1 S/m) and mechanically strong, and they exhibit excellent electrochemical performance. It is believed that the synergy effect of hydrophobic and π–π interactions between graphene sheets, which are increased after chemical reduction, caused the 3D assembly of the flexible graphene sheets and produced sucha high-performance graphene-based hydrogel. Consequently, the specific capacitance of graphene hydrogel was measured to be up to about 240 F/g at a discharge current density of 1.2 A/g, in 1 M aqueous solution of H_2SO_4. In another report from Shi's research group,[90] they reported that 2-aminoanthraquinone (AAQ) molecules can be covalently grafted onto chemically modified graphene (CMG), and AAQ-functionalized CMG sheets (AQSGH) were able to self-assemble into macroporous hydrogels. Although the conductivity is relatively low for AQSGH (~0.3 S/m), the SSA of AQSGH was measured to be as large as 1050±60 m^2/g, and a high specific capacitance of 258 F/g was achieved at a discharge current density of 0.3 A/g in 1 M aqueous solution of H_2SO_4 for the AQSGH-based supercapacitor electrodes. It was believed that this high capacitance is mainly due to the covalently bonded AAQ moieties contributing additional redox capacitance. Moreover, the AQSGH electrode exhibited an excellent cycling stability and no decrease upon charge/discharge treatment after 2000 cycles. Instead, it was found that the cycling stability slightly increased, possibly due to the fact that the wettability and electrochemical activity of the electrode were improved.

To further improve the conductivity of the graphene-based hydrogel, Shi and co-workers[91] prepared another kind of graphene hydrogels via hydrothermal reduction of graphene oxide dispersions followed by further reduction with hydrazine or hydroiodic acid. The chemically reduced graphene hydrogels exhibited relatively high conductivities of 1.3–3.2 S/m. Accordingly, the graphene-based hydrogel reduced by 50% hydrazine at 100 °C for 8 h was found to be the best electrode material with a high specific capacitance of 220 F/g at a current density of 1 A/g. Remarkably, this capacitance can be maintained for about 74% as current density was increased up to 100 A/g. Furthermore, the capacitor displayed a power density of 30 kW/kg and an energy density of 5.7 kW/kg at a current density of 100 A/g. It also showed a long cycle life along with ~92% capacitance retention after 2000 cycle tests at a moderate current density of 4 A/g. It is considered that this excellent supercapacitor performance is mainly because of the relatively high conductivity as well as the unique 3D macroporous structure of this graphene-based hydrogel.

3.4. Graphene-Based Electrode Materials Prepared through Activated Graphene

Activation has been extensively used to obtain porous carbon-based materials for the application of supercapacitor electrodes.[92–95] One of the most widely used activation method for the carbon-based materials is electrochemical activation.[96,97] It has been reported that during electrochemical activation, the original carbon precursor material with a small surface and a rather small capacitance can develop a significant improvement in capacitance. Hence, this technique is also supposed to enhance the performance of graphene-based supercapacitor electrodes. In the work published by Kotz and co-workers,[98] the electrochemical activation of partially reduced GO was synthesized and their supercapacitor performance was investigated. The initial specific capacitance of the partially reduced GO, which was prepared by thermal reduction, was negligibly small due to their very low BET specific surface area of about 5 m^2/g. However, after electrochemical activation, the activated graphene-based materials, which had a very large surface area of 2687 m^2/g (close to the theoretical surface area of graphene), displayed a specific capacitance up to 220 F/g (scan rate: 1 mV/s) in standard organic 1 M Et_4NBF_4 in acetonitrile electrolyte. It is considered that the clear dependence of the activation potential of partially reduced GO on the lattice spacing indicates that the electrochemical activation is, at least in part, related to ion and/or solvent intercalation.

In addition to electrochemical activation, Pan and co-workers[99] recently developed a way to chemically modify graphene sheets by KOH to enhance the supercapacitaor capacity of graphene-based materials. After modifying the graphene nanosheets by using concentrated KOH solution, this graphene-based material showed a specific capacitance of 136 F/g at the scan rate of 10 mV/s in 1 M Na_2SO_4 aqueous solution, which was about 35% higher than the pristine graphene nanosheets. This increased capacity is thought to be a result of edge defects and the oxygen-containing groups introduced by the KOH modification, which not only increased the accessibility of the graphene nanosheets by the electrolyte ions, but also led to further pseudo-capacitive effects.

Significantly, Ruoff and co-workers[100] reported a simple activation with KOH of microwave-exfoliated GO (MEGO) and thermally exfoliated GO, to achieve SSA values of up to

small 2012,
DOI: 10.1002/smll.201102635

small NANO MICRO

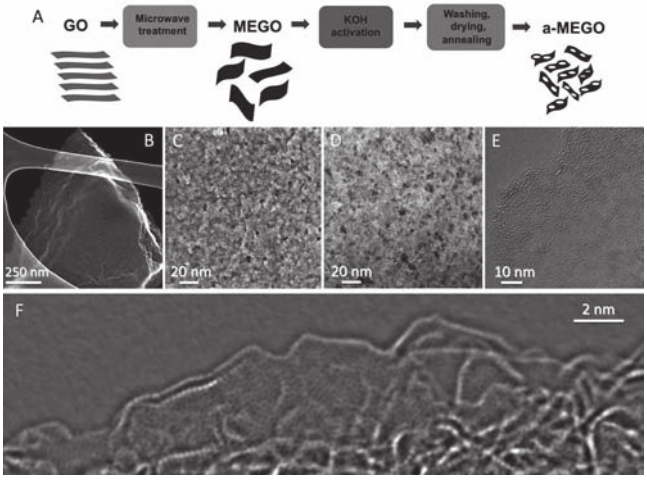

Figure 7. Graphene-based electrode materials prepared by activation of microwav-exfoliated GO. A) Schematic showing the microwave exfoliation/reduction of GO and the following chemical activation process. B) Low-magnification SEM image of a 3D MEGO fragment. C) High-resolution SEM image of a different sample region. D) Annular dark field scanning transmission electron microscopy (ADF-STEM) image of the same area as in (C), acquired simultaneously. E) High-resolution phase- contrast electron microscopy image of the thin edge of a MEGO fragment. Reproduced with permission.[100] Copyright 2011, the American Association for the Advancement of Science.

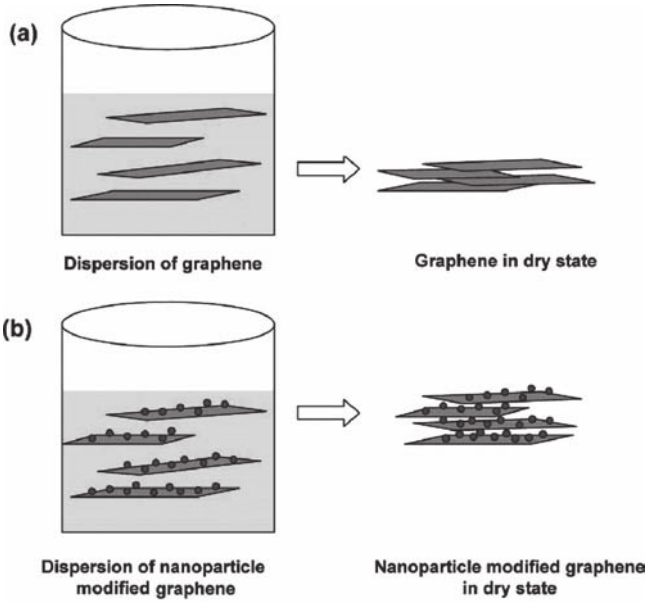

Figure 8. Schematic of a) graphene sheets and b) nanoparticle-modified graphene sheets in its dispersion and dry state. Reproduced with permission.[69] Copyright 2008, American Chemical Society.

3100 m^2/g (**Figure 7**). It is found that the activation process etches the MEGO and generates a 3D distribution of what are referred to as mesopores. Remarkably, the activation with KOH yields a continuous 3D network of pores of extremely small size, ranging from <1 to 10 nm. Furthermore, although the graphene sheets bend through high degrees of curvature, the in-plane crystallinity is preserved. The supercapacitor performance of the activated-MEGO (SSA = ~2400 m^2/g) in 1-butyl-3-methyl-imidazolium tetrafluoroborate/acetonitrile (BMIM BF_4/AN) electrolyte was thus measured and yielded a specific capacitance of above 166 F/g as obtained at a current density of up to 5.7 A/g. Using the working voltage of 3.5 V, the energy density was calculated to be about 70 W h/kg, and the power density was also very high at ~ 250 kW/kg, as estimated by using the voltage drop and electron spin resonance (ESR) obtained from the discharge curve. Moreover, the activated-MEGO showed very impressive cycling stability, such that after 10 000 constant current charge/discharge cycles at a current density of 2.5 A/g in neat BMIM BF_4 electrolyte, 97% of its capacitance was still retained. On the grounds of these excellent results, it is believed that this simple activation process, which is already commercially demonstrated for activated carbons (ACs), may allow the scale up of the production of activated-graphene-based materials for high-performance energy storage devices within a short period.

3.5. Graphene-Based Electrode Materials Prepared through Intercalated-Graphene-Based Sheets

It was well known that after the chemical reduction of GO in the aqueous solution, the substantial loss in oxygen-containing groups of GO would seriously lower the electrostatic repulsions between GO sheets, leading the reduced graphene oxide (RGO) to agglomerate. This agglomeration not only decreases the surface area, but also precludes the access of electrolyte ions to the surface of the RGM sheets,[101] resulting in limited supercapacitor performance. Thus, many reports have involved incorporating "stabilizer" or "spacers" into the graphene layers to inhibit the agglomeration of reduced graphene sheets. As a result, the existence of "stabilizer" or "spacers" not only can improve the electrolyte–electrode accessibility in the supercapacitors, but can also ensure the high electrochemical utilization of graphene sheets as well as the open nanochannels provided by 3D hybrid material.[102]

Samulski and co-workers[69] reported a (platimun nanoparticle)–graphene composite with a partially exfoliated graphene morphology derived from drying aqueous dispersions of Pt nanoparticles adhered on graphene sheets (**Figure 8**). The Pt nanoparticles that acted as spacers can prevent the face-to-face aggregation of graphene sheets and thus result in mechanically jammed, exfoliated graphene sheets with a very high surface area of about 862 m^2/g, which made this graphene–Pt hybrid a very promising electrode material for supercapacitors. While the dried graphene gives a capacitance of 14 F/g, the Pt–graphene hybrid has a significantly larger capacitance of 269 F/g.

In another work, Kar and co-workers[103] presented a scalable and facile technique for noncovalent functionalization of graphene with 1-pyrenecarboxylic acid (PCA) that directly exfoliates single-, few-, and multilayered graphene flakes into stable aqueous dispersions, as shown in **Figure 9**. As spacer materials, PCA initially served as a "molecular wedge" that cleaves the individual graphene flakes from the raw graphite pieces, and then formed stable polar functional groups on the graphene surface via a noncovalent π–π stacking mechanism

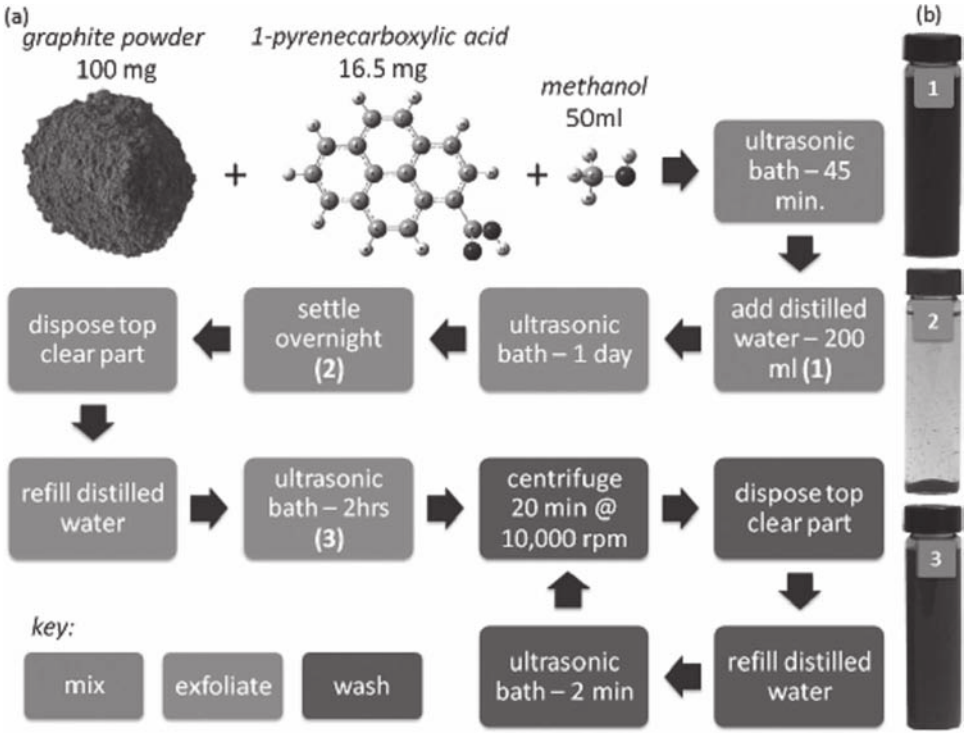

Figure 9. Schematic of exfoliation of graphene from graphite powder. a) Process flow with different steps (mixing, exfoliation, and washing). b) Digital photographs of vials containing the dispersion at stages 1–3 (as indicated in (a)). Reproduced with permission.[103] Copyright 2010, American Chemical Society.

which would not destroy its sp^2 hybridization. This procedure made the PCA–graphene composites have high conductivity and a surface area suitable for supercapacitor electrode materials. Specific capacitance values as high as 120 F/g in 6 M KOH solution with impressive power densities (~105 kW/kg) and energy densities (~9.2 W h/kg) are obtained. Furthermore, they found that operating without distortion at high scan rates of up to 1000 mV/s and even after 1000 charge/discharge cycles without the use of any binders or specially prepared current collectors, the ultracapacitors show a comparable supercapacitor performance with that of previously reported graphene-based ultracapacitors, and they are substantially better than those obtained with carbon nanotubes.[38]

Wu and co-workers[104] utilized different kinds of surfactants (tetrabutylammonium hydroxide (TBAOH), cetyltrimethylammonium bromide (CTAB), and sodium dodecylbenzene sulfonate (SDBS) to intercalate and stabilize graphene oxide, followed by reduction using hydrazine, to prepare a series of surfactant-stabilized graphene materials used for supercapacitor electrodes. In addition to stabilizing the morphology of single- or few-layer structures of graphene sheets during reduction, the presence of surfactants in graphene materials can also enhance the wettability of the graphene surface and thus improve its performance as a supercapacitor electrode. It was found that when exploiting TBAOH as stabilizer, the graphene–TBAOH had the best supercapacitor performance. The highest specific capacitance of 194 F/g was obtained from TBAOH-stabilized graphene at a specific current density of 1 A/g in 2 M H_2SO_4 electrolyte. Furthermore, when the current density was increased to 5 and 10 A/g, high specific capacitances at 180 and 175 F/g, respectively, were obtained for the graphene–TBAOH hybrid, which are highly desirable for fast charging/discharging supercapacitors.

Additionally, carbon-based nano- or microaterials can be used as useful spacer materials. Fan and co-workers[102] prepared graphene–(carbon black) composites through the facile method of ultrasonication and in situ reduction of GO. As the spacers, carbon black (CB) particles can inhibit the agglomeration of graphene sheets and thus improve electrolyte–electrode accessibility. On the other hand, it has been reported that the capacitance of the edge orientation of graphite is an order of magnitude higher than that of the basal layer.[30,42] The CB particles are mainly deposited on the edge surface of the sheets for graphene–CB hybrids; hence, the electrolyte ions' diffusion and migration into graphene–CB hybrid are easily during the rapid charge/discharge process. The specific capacitance of 175 F/g is obtained at 10 mV/s in 6 M KOH aqueous solution for this graphene–CB hybrid. Even at a scan rate of 500 mV/s, the graphene–CB hybrid still showed a specific capacitance of 118 F/g. Moreover, after 6000 cycles, the capacitance decreases to only 9.1% of the initial capacitance indicating that the graphene–CB hybrid electrode displayed excellent cycle stability and a very high degree of reversibility in the repetitive charge/discharge cycling.

In addition to carbon black, mesoporous carbon spheres were also used to intercalate between graphene sheets to

small 2012,
DOI: 10.1002/smll.201102635

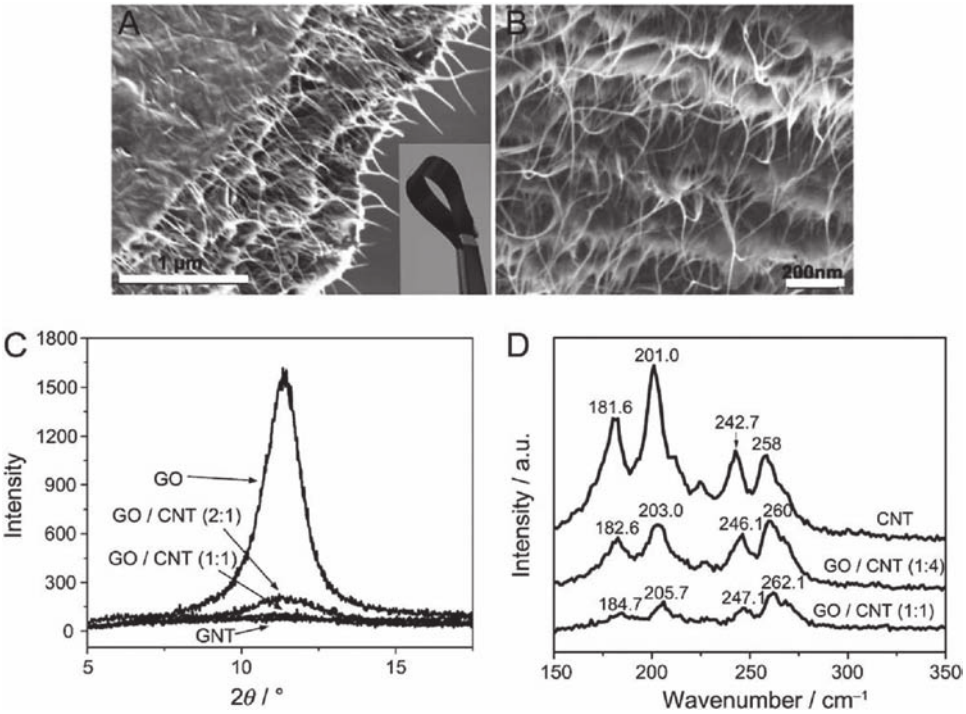

Figure 10. Graphene–CNT hybrids for supercapacitor applications. A,B) SEM images of the resulting GO/CNT hybrid film. The inset in (A) shows a bent strip of the resulting film. C,D) XRD patterns and Raman spectra of the GO/CNT films with various weight ratios of GO and CNTs. Reproduced.[108]

construct 3D carbon-based architectures by Zhao and co-workers[101] In the preparation process, negatively charged GO sheets first strongly interacted with positively charged mesoporous silica spheres (MSS) to form a MSS–GO composite. Then, the MSS were then used as a template for replicating mesoporous carbon spheres (MCS) via a chemical vapor deposition process, followed by removal of the silica spheres. During the CVD process, the GO sheets were reduced to RGM in the meantime. The intercalation of MCS indeed can prevent graphene sheets from serious agglomeration. Moreover, a good contact between porous MCS and graphene sheets also favored charge propagation within the electrode. Based on the N_2 adsorption data, a high BET surface area of 1496 m^2/g and a total pore volume of 3.36 cm^3/g were determined for this (graphene-based material)–(carbon sphere), GMCS, composite. The specific capacitance of 171 F/g is obtained for this GMCS electrode at a scan rate of 10 mV/s. Furthermore, about 94% specific capacitance was preserved after 1000 galvanostatic charge/discharge cycles, showing a good cyclability of the GMCS-based carbon electrode.

For the purpose of energy storage applications, it is highly desirable to use 1D carbon nanotubes (CNTs) as spacers to separate 2D graphene-based sheets to preserve graphene's high surface area and exploit the high conductivity for CNTs to increase the conductivity of these carbon-based hybrids.[105–107] However, since both the as-produced graphene and CNTs are generally in an agglomerated powder form, a suitable technique is needed to mix or disperse these two kinds of carbon-based nanomaterials in order to realize the chemical and physical synergies of their hybrids. In a recent work, Li and co-workers[108] explored graphene oxide as a dispersant to suspend the unfunctionalized CNTs in aqueous solution and to develop a new solution processing strategy for making graphene–CNT hybrids for the supercapacitor applications (**Figure 10**). The oxygen-containing groups rendered GO sheets hydrophilic and highly dispersible in water, whereas the aromatic regions offered active sites to make it possible to interact with the aromatic molecules of CNTs through π–π supramolecular interactions. Electrophoresis experiments were carried out to confirm that the CNTs were indeed strongly attached to the negatively charged GO nanosheets. Although the GO nanosheets are insulators, the electrical conductivity of the hybrid films can be increased after the electrochemical treatment. While the measured specific capacitance for the graphene-only electrode was about 140 F/g at a current density of 0.1 A/g; it dropped to 30 F/g at a current density of 30 A/g. Significantly, supercapacitors based on the electrochemically reduced GO and carbon nanotubes (ER-GO/CNT) (1:1) exhibited a specific capacitance of over 90 F/g at a high current density of 100A/g due to the effective synergies of the graphene-based materials and CNTs.

In another work, Dai and co-workers[109] utilized an electrostatic self-assembly method to fabricate the graphene–CNT hybrid films. Stable aqueous dispersions of polymer-modified graphene sheets were first prepared via in situ reduction of GO nanosheets in the presence of cationic poly(ethyleneimine) (PEI), and then the resultant water-soluble PEI-modified graphene sheets were used for sequential self-assembly with acid-oxidized multiwalled

DOI: 10.1002/smll.201102635

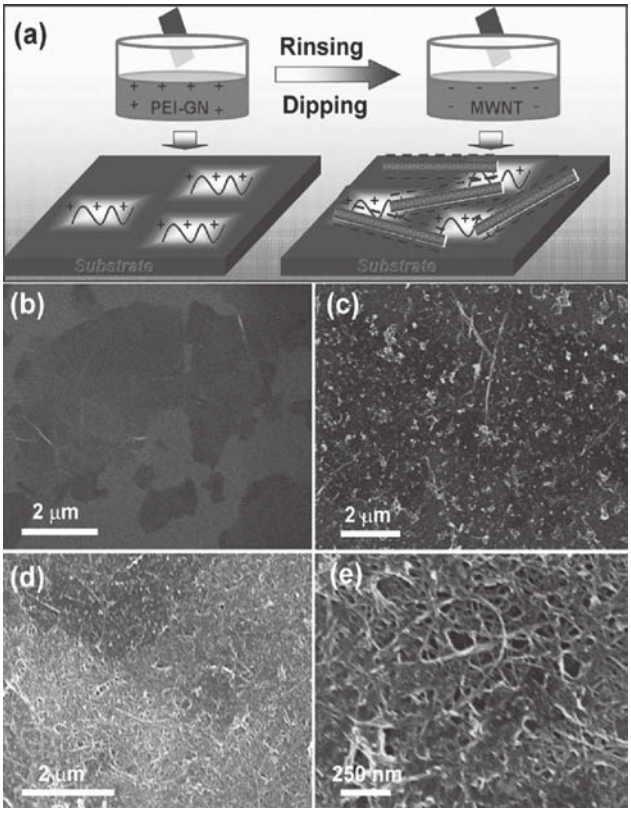

Figure 11. Graphene–CNT hybrid films prepared by electrostatic self-assembly method. a) Illustration of positively charged PEI–graphene nanosheets (GN) and negatively charged MWNT film deposition process. SEM images of b) the first layer PEI–GN and c) the first bilayer $[PEI–GN/MWNT\text{-}COOH]_1$ film deposited on a silicon substrate. d,e) SEM images of the $[PEI–GN/MWNT\text{-}COOH]_9$ film after the ninth deposition cycle under different magnifications. Reproduced with permission.[109] Copyright 2009, American Chemical Society.

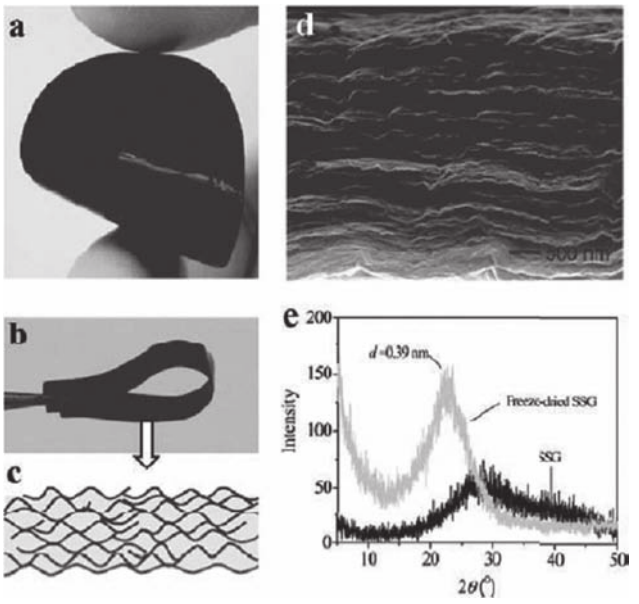

Figure 12. Characterization of self-stacked solvated graphene (SSG) films. a,b) Photographs of the as-formed flexible SSG films. c) Schematic of the cross-section of SSG film. d) SEM image of the cross-section of a freeze-dried SSG film. e) XRD patterns of as-prepared and freeze-dried SSG films. Reproduced.[111]

carbon nanotubes (MWNTs) to form hybrid carbon films (**Figure 11**). These hybrid films possessed an interconnected network of carbon structures with well-defined nanopores for fast ion diffusion, which makes these hybrid films highly promising for supercapacitor electrodes. The shape of the cyclic voltammogram of this graphene–CNT hybrid electrode was quite rectangular, indicating potential for supercapacitor applications. Moreover, even at an exceedingly high scan rate of 1 V/s, an average specific capacitance of 120 F/g was still obtained for this graphene–CNT hybrid films.

Zhang and co-workers[110] reported the fabrication of a flexible graphene–MWNT film via a flow-directed assembly technique from a suspension of GO and pristine MWNTs followed by the use of gas-based hydrazine to reduce the GO to graphene sheets. The as-prepared flexible graphene–MWNT film was used to make flexible supercapacitors directly, without the insulating binder. It was confirmed that this flexible film had a layered structure with MWNTs homogeneously dispersed among the graphene nanosheets. The MWNTs in the hybrid films not only can separate the graphene sheets, bus can also bridge the defects for electron transfer between the graphene sheets, increasing the electrolyte–electrode contact area and facilitating transportation of electrolyte ions and electrons into the inner region of electrode. Thus, these flexible graphene–MWNT films had a high specific capacitance of 256 F/g at the current density of 0.1 A/g and a good rate capability (49% capacitance retention at 50 A/g). Moreover, outstanding stability of the specific capacitance—97% retention after 2000 charge/discharge cycles—was obtained for this flexible electrode, indicating promising potential in its application in flexible energy storage devices.

More recently, Li and co-workers[111] investigated an interesting strategy, in which water is the "spacer" in an ordered fashion within pre-synthesized graphene sheets. They prepared graphene-based electrodes based on this low-temperature, liquid-phase, and bottom-up assembly technique. Inspired by the fact that biological tissues need to remain in a proper hydrated state since birth, they utilize water as an effective "spacer" to prevent the re-stacking of chemically converted graphene (CCG) sheets (**Figure 12**). Due to the presence of hydrophilic groups on the surface, water can be absorbed on the CCG surface quite tightly to induce repulsive hydration forces between sheets. The resultant self-stacked solvated graphene (SSG) film displayed unprecedented electrochemical performance: a specific capacitance of up to 215.0 F/g was obtained in an aqueous electrolyte, and a capacitance of 156.5 F/g can be reached even when the supercapacitor is operated at an ultrafast charge/discharge rate of 1080 A/g. The SSG film can provide a maximum power density of 414.0 kW/kg at a discharge current of 108 A/g. Additionally, the solvent graphene exhibited excellent cyclability: over 10 000 cycles, it can retain over 97% capacitance even under a high operation current of 100 A/g. Importantly, the water in the solvent graphene sheets can be easily exchanged with other solvents,

DOI: 10.1002/smll.201102635

NANO MICRO small

such as ionic liquids. After exchanged with 1-ethyl-3-methylimidazolium tetrafluoroborate, this graphene-based supercapacitor can exhibit a specific capacitance of up to 273.1 F/g and an energy density and maximum power density up to 150.9 W h/kg and 776.8 kW/kg, respectively.

3.6. Graphene-Based Electrode Materials Prepared through Other Novel Techniques

The functional groups on the surface of GO allow it to be facilely homogeneously dispersed in solution. However, these defects also severely affect the intrinsic properties of graphene, such as conductivity, which is highly important for the supercapacitor electrode. The use of graphene nanosheets prepared by direct exfoliation from graphite powder as opposed to that from GO gives rise to a graphene-based material without severely destroying the native and excellent features and aromatic structure of graphene sheets.[61] Drzal and co-workers[112] employed a capillary-driven self-assembly monolayer of graphene nanosheets, which they prepared through direct exfoliation in organic solvent,[113] to create a highly aligned multilayer structure over a large macroscopic area (**Figure 13**). This method can deposit graphene nanosheets on a stainless steel plate, which can be used as binder-free supercapacitor electrode directly. To achieve the purpose of enhancing the capacitance, they combined the large and small graphene nanosheets in an aligned conformation. The large nanosheets not only can contribute to the double-layer capacitance, but they can also act as current collectors within the bulk electrode structure for facile electronic conduction from the internal structure to the current collector surface. The high-surface-area, small nanosheets on the other hand enhance the specific capacitance by creating a highly mesoporous network and improving the wettability of the electrodes resulting from the presence of oxygen-containing functional groups present at the edges. Therefore, the average specific capacitance of the aligned composite configuration reached close to 80 F/g at a very high current density of 10A/g. Furthermore, the high electrochemical cyclic stability of this multilayer film electrode was evidenced from the retention of more than 98% of the specific capacitance at the end of 1000 electrochemical cycles.

In another recent work, Ning and co-workers[114] utilize a template CVD approach to produce nanomesh graphene with well-controlled structure on the gram scale (**Figure 14**). By exploiting porous MgO layers with polygonal shapes as a template, the nanomesh graphene could be produced to have only one to two graphene layers, polygonal morphologies, and large specific surface areas up to 1654 m^2/g with good structural stability. The specific capacitance of 245 F/g was obtained at a constant current density of 1 A/g in 6 M KOH aqueous solution for this nanomesh graphene. Furthermore, the nanomesh graphene electrode showed an excellent long cycle life with 94.1% specific capacitance retained after 2000 cycles.

Due to its combining and outstanding properties such as remarkable mechanical strength, high conductivity, high flexibility, unique optical transparency, large surface area, and 2D one-atom-thick structure, graphene can be used to fabricate graphene-based ultrathin, transparent, and flexible supercapacitors. Yu and Chen and co-workers[115] reported that the ultrathin films were prepared through vacuum filtration of graphene solution, followed by transferring the graphene films onto glass, a poly(ethylene terephthalate) (PET) substrate, or glassy carbon electrode (**Figure 15**). The capacitance obtained from charge/discharge analysis was 135 F/g for a graphene-based film of approximately 25 nm which had

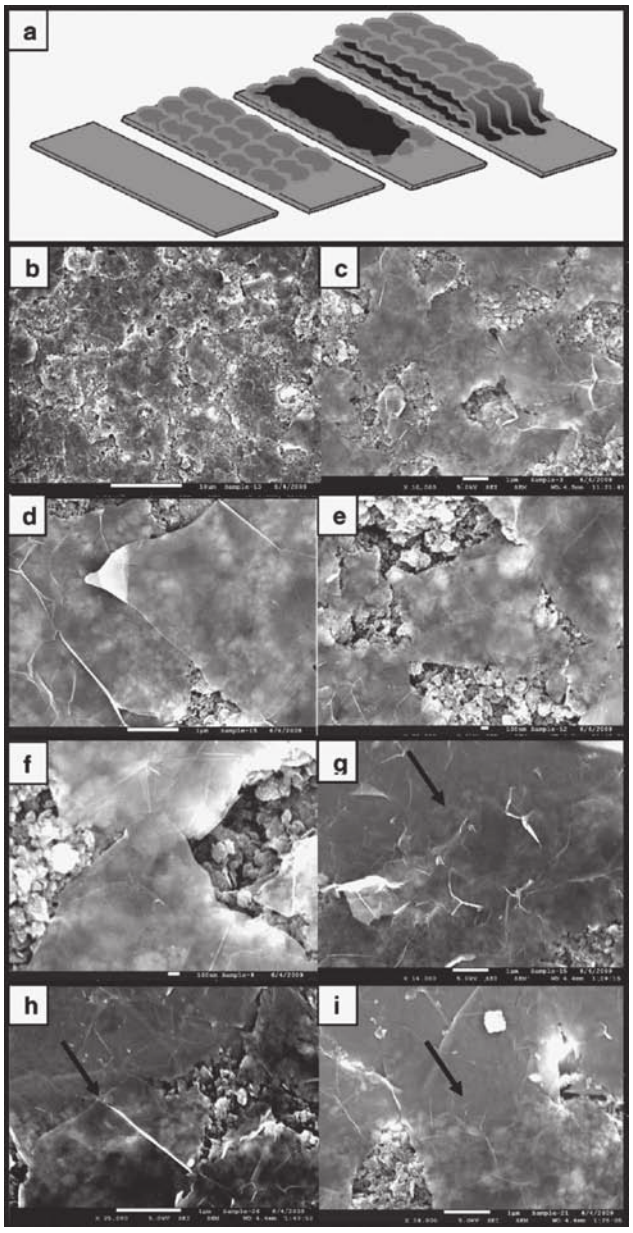

Figure 13. Fabrication of aligned composite of large and small nanosheets. a) Schematic of the development of layered structure. b–f) Field-effect (FE) SEM characterization showing a monolayer coverage of a large nanosheet placed on top of smaller nanosheets, where the large ones are individually connected with each other near their edges. g–i) Large nanosheets connecting the bulk electrode to the top section where it is attached on the current collector surface. Reproduced with permission.[112] Copyright 2010, American Chemical Society.

DOI: 10.1002/smll.201102635

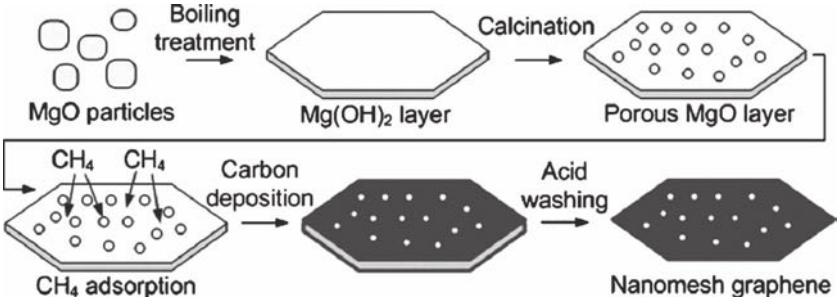

Figure 14. Illustration of the formation of the polygonal nanomesh graphene. Reproduced with permission.[114] Copyright 2011, Royal Society of Chemistry.

a transmittance of 70% at 550 nm and a high power density of 7200 W/kg in 2 M KCl electrolyte. It is suggested that the light-weight architecture efficiently employs graphene materials to facilitate a minimal diffusion length for electrolyte ions to access the active material while improving the charge transport kinetics resulting in a high energy and power density electric double-layer capacitor.

Furthermore, it has been studied that inkjet printing is a useful approach to prepare graphene thin-film-based electronic devices. Accordingly, Lee and co-workers[116] reported for the first time the feasibility of inkjet-printing a GO aqueous solution directly on Ti foils and then subsequently using thermal reduction as a new avenue for fabricating graphene-thin-film-based supercapacitor electrodes. The specific capacitance of these electrodes decreased from 125 to 121 F/g over 1000 CV cycles at a constant scan rate of 50 mV/s demonstrating 96.8% capacitance retention. In another interesting work, Ajayan and co-workers[117] demonstrated the utilization of pristine and multilayer graphene as electrodes in a novel "in-plane" device geometry for use in supercapacitors, as depicted in **Figure 16**. Compared to the conventional stacked geometry, it is considered that this favorable in-plane design offers three opportunities to improve the performance of this graphene-based supercapacitor: 1) the electrolyte ions may enhance the interaction with all the carbon layers (Figure 16a), leading to a full utilization of the high surface area offered by the graphene layers; 2) the graphene-based 2D architecture also allows for employing the unique electrochemical properties of graphene edges along with the basal planes of graphene; 3) this 2D in-plane design allowed the possibility of extreme miniaturization of device thickness (e.g., single-layer graphene devices). As a result, the best capacitance value of this novel graphene-based 2D "in-plane" supercapacitors was up to 250 F/g, and the normalized capacitance reached 394 μF/cm^2, higher than the previously reported 300 μF/cm^2.[118]

3.7. The Effect of the Electrolyte

A main issue with the carbon-based supercapacitor electrode materials is that the entire surface area is not electrochemically accessible by an electrolyte. This has been attributed to the following facts: i) a small micropore size (pore size <2 nm) in porous carbon results in the low rate of molecular or ionic transport through the pores, and ii) a hydrophobic graphite-like surface provides low coverage that is accessible for the formation of a double layer.[119,120]

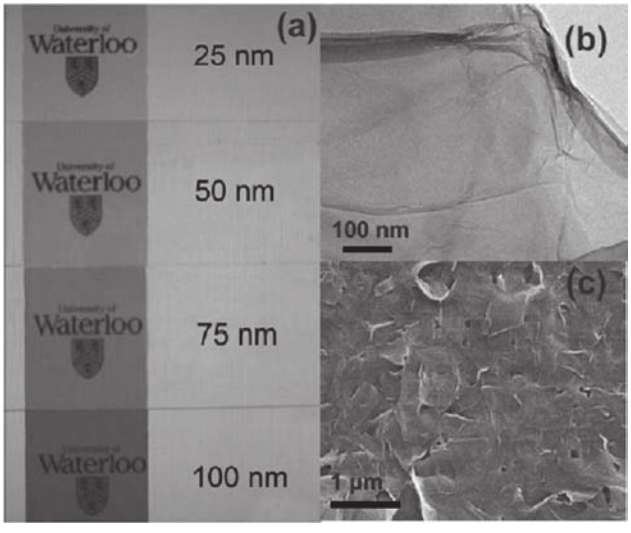

Figure 15. Ultrathin films prepared by filtration of graphene solution. a) Photographs of transparent thin films of varying thickness on glass slides. b) TEM image of graphene collected from dispersion before filtration. c) SEM image of graphene film on glass slide. Reproduced with permission.[115] Copyright 2010, American Institute of Physics.

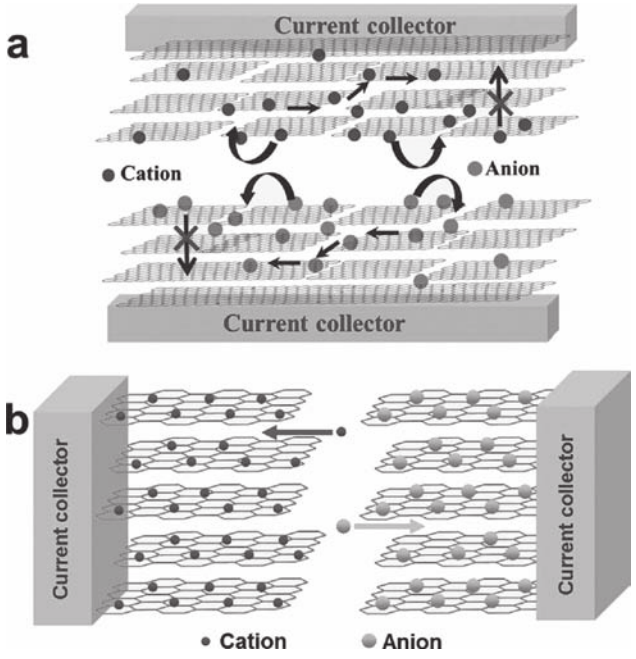

Figure 16. a) Schematic depiction of the stacked geometry used for the fabrication of supercapacitor devices. b) Schematic depiction of the operating principle in case of the in-plane supercapacitor device utilized for the performance evaluation of graphene as electrodes. Reproduced with permission.[117] Copyright 2011, American Chemical Society.

DOI: 10.1002/smll.201102635

small NANO MICRO

These drawbacks also restrict the applications of graphene-based materials as electrodes in supercapacitors. Hsieh and co-workers[121] thus studied the surface accessibility of GO sheets using different electrolytes, such as Li_2SO_4 and Na_2SO_4. This work adopted a filtration technique to prepare GO stacking layers with a high oxidation level on carbon paper forming a flexible electrode for supercapacitors. The GO sheets were still occupied by oxygen-containing groups and generated highly oxidized basal planes and edges. It is interesting to find that GO-based capacitors displays specific capacitances of 238.0 and 98.8 F/g in Li_2SO_4 and Na_2SO_4 electrolytes, respectively. The difference of diffusivities in GO sheets between the Li^+ and Na^+ ion have been considered to be the reason for this difference in the capacitance results. Because 1) Li^+ is smaller than Na^+ and 2) the hydrated Li^+ ion forms dual layers, whereas the hydrated Na^+ ion possibly prefers monolayer adsorption on the GO sheets, the diffusion coefficient of Li^+ is three times higher than that of Na^+ in the GO-based supercapacitors. Accordingly, this work has shed some light on how electrolyte type affects the electrochemical performance of GO-based supercapacitors, favoring the fundamental properties of capacitive behavior on graphene-based materials.

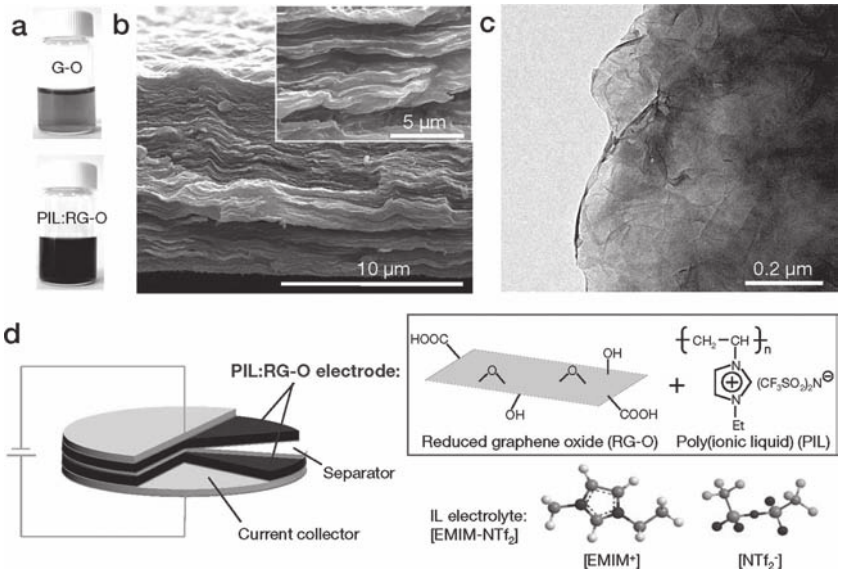

Figure 17. Poly(ionic liquid)-modified reduced graphene oxide (PIL:RGO) electrode materials. a) Optical images of graphene oxide (GO) in propylene carbonate (PC) and PIL:RGO in PC. b) SEM and c) TEM image of PIL:RGO platelets. d) Schematic diagram of the supercapacitor based on the PIL:RGO electrodes and ionic liquid electrolyte (EMIM-NTf_2). Reproduced with permission.[123] Copyright 2011, American Chemical Society.

Additionally, supercapacitors can be coupled with fuel cells or batteries to deliver the high power needed during acceleration and to recover the energy during braking. However, a major shortcoming of current supercapacitors is their low energy density (typically 5–10 W h/kg), which is significantly lower than the 20–35 W h/kg of lead-acid, the 40–100 W h/kg of Ni metal hydride, and the 120–170 W h/kg of lithium-ion.[122]

Owing to the limited potential of 1 V in aqueous solution, employing other nonaqueous electrolytes to overcome this narrow electrochemical window is a key issue in the development of high-performance supercapacitors. Conventional organic electrolytes, such as tetraethylammonium tetrafluoroborate and triethylmethylammonium tetrafluoroborate in acetonitrile, have been applied to fabricate supercapacitors with a relatively wide potential window.[71] Nevertheless, organic electrolytes suffer from the drawbacks involving electrolyte depletion upon charge, narrow operational temperature range, and low safety. Therefore, ionic liquids have been used to replace organic electrolytes in a wide range of applications. Their winning properties, including high ionic conductivity, wider electrochemical window (up to 7 V), excellent thermal stability (–40 to +200 °C typical), nonvolatility, nonflammability, and nontoxicity, make them excellent electrolytes for various electrochemical systems.[122] Rao and co-workers[35] were the first to use an ionic liquid with graphene-based materials, which were prepared by high-temperature exfoliation, to fabricate supercapacitors. However, due to the relatively low obtained specific capacitance (75 F/g), an energy density of only 31.9 W h/kg at 5 mV/s and 60 °C was gained. To further improve the compatibility between graphene-based materials and ionic liquid electrolytes, Suh and co-workers[123] incorporated a poly(ionic liquid)-modified reduced graphene oxide (PIL:RGO) electrode and an ionic liquid (IL) electrolyte (specifically, 1-ethyl-3-methylimidazolium bis(trifluoromethylsulfonyl)amide or EMIM-NTf_2) to develop a high-performance supercapacitors (**Figure 17**). These PIL-modified reduced GO materials offer advantages for supercapacitor applications in that they could provide enhanced compatibility with certain IL electrolytes and improve the accessibility of IL electrolyte ions into the graphene electrodes. As a result, a supercapacitor assembled with such a PIL:RGO electrode and with EMIM-NTf_2 as the electrolyte exhibited a specific capacitance of 187 F/g. Nevertheless, the energy density is still low, and a maximum energy density of only 6.5 W h/kg with a maximum power density of 2.4 kW/kg was also obtained.

Recently, Jang and co-workers[122] reported results of a study on a mesoporous graphene structure that is accessible for ionic liquid electrolytes and, thus reaches an exceptionally high EDL capacitance and an unprecedented high level of energy density even though ionic liquids have large molecules and high viscosity. They prepared curved graphene sheets by injecting a GO aqueous solution into a forced conventional oven in which a stream of compressed air was introduced to produce a fluidized-bed situation. Upon removal of the solvent or liquid, the desired curved graphene sheets were obtained. This curved graphene sheet morphology (**Figure 18**) is capable of preventing graphene sheets from closely re-stacking with one another when they are packed or compressed into an electrode structure, which results in maintaining a mesoporous structure with pore

DOI: 10.1002/smll.201102635

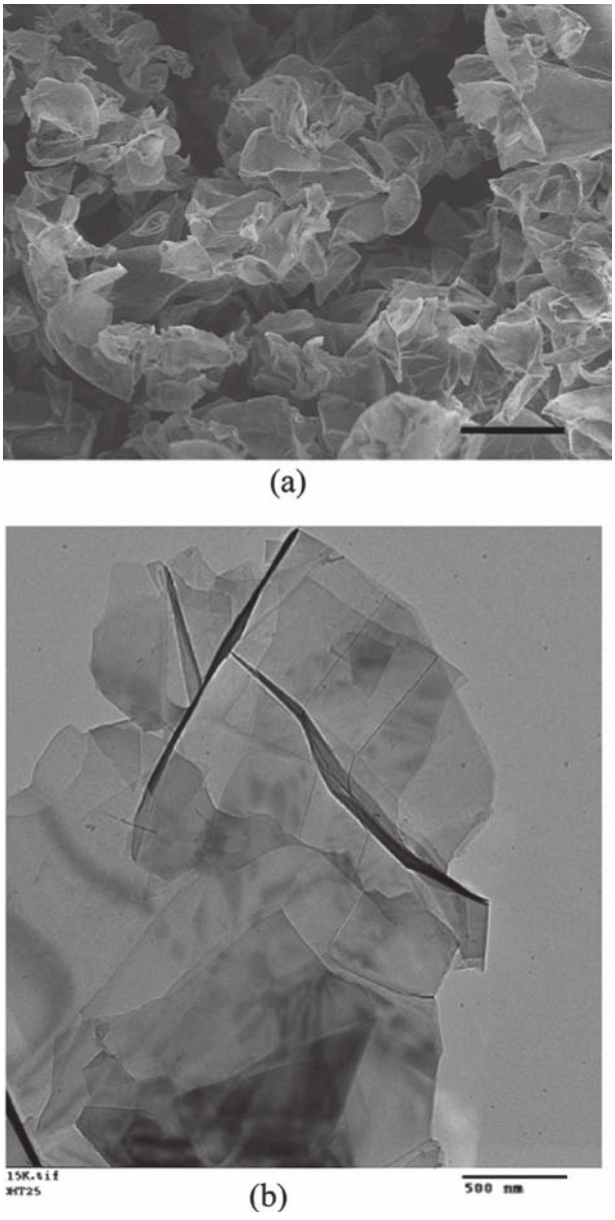

Figure 18. Morphology of curved graphene sheet. a) SEM image of curved graphene sheets, b) TEM image of flat graphene sheets prepared by a conventional chemical route (scale bar 500 nm). Reproduced with permission.[122] Copyright 2010, American Chemical Society.

sizes in the range of 2 to 25 nm. The specific capacitances of curved graphene-based supercapacitors in an ionic liquid are typically 100–250 F/g at a high current density of 1 A/g with a discharge voltage of 4.0 V. Furthermore, the shape of the cyclic voltammogram is nearly rectangular, indicating the ideal double-layer capacitor behavior and no major pseudo-capacitance contribution. Importantly, the ionic liquid, EMIM BF_4, can work at a voltage of up to 4.5 V, leading to an excellent energy density of 85.6 W h/kg at 1 A/g at room temperature (or 136 W h/kg at 80 °C), which is comparable to that of a modern nickel metal hydride battery used in a hybrid vehicle.[122] This breakthrough energy storage device is possible attributed to the high intrinsic capacitance and the exceptionally high specific surface area of curved graphene sheets that can be readily accessed and wetted by an ionic liquid electrolyte capable of operating at a high voltage.

4. Graphene-Conducting Polymer-Composite-Based Pseudo-capacitors

4.1. Electrode Materials Based on (Graphene Oxide)–PANI Composites

Conductive polymers (CPs) have been widely studied in supercapacitors due to their very high pseudo-capacitance. Accordingly, the main conductive polymer materials that have been investigated for the supercapacitor electrode are polyaniline (PANI),[124] polypyrrole (PPY),[125] polythiophene (PTH), and their derivatives.[126] Among these polymers, PANI is considered the most promising material because of its high capacitive characteristics, low cost, and ease of preparation.[127,128] Nevertheless, the relatively poor cycling life and stability severely restrict its practical applications.[129] In contrast, carbon-based materials, such as activated carbon (AC), mesoporous carbon (MC), and carbon nanotubes (CNTs) usually exhibit good stability, but the capacitance values are relatively low due to the limited active surface in the materials.[40,130,131] Consequently, composite materials comprising carbon-based materials such as CNTs and conducting polymers such as PANIs have been investigated as supercapacitor electrodes, and high capacitances and improved stability have been achieved[132,133] due to the synergetic combination of the excellent conducting and mechanical properties of CNTs and the high pseudo-capacitance of the PANIs. However, the high cost as well as relatively low electric double-layer capacitance (only up to 80 F/g) restricts the practical application of pristine CNTs.[44,134] Graphene has thus been applied for preparing composites with CPs to be used as supercapacitor electrodes, owing to its many excellent and unique features.

Hao and co-workers[135] reported a novel kind of electrode material based on fibrillar PANI doped with graphene oxide sheets, which was synthesized via in situ polymerization of the monomer in the presence of graphene oxide. Its specific capacitance was up to 531 F/g, which is much higher than pure PANI, indicating the synergistic effect between GO and PANI. In another work of Hao's group,[129] they further investigated the effect of raw graphite material sizes and feeding ratios on the electrochemical properties of the GO–PANI composites. They found that the morphology of the prepared composites is influenced dramatically by the different mass ratios. These composites are proposed to be combined through a) an electrostatic interaction (doping process), b) hydrogen bonding, and c) π–π stacking interactions. The highest specific capacitances of 746 F/g (12 500 mesh of pristine graphite powder) and 627 F/g (500 mesh of pristine graphite powder) corresponding to the mass ratios of1:200 and 1:50 (graphene oxide/aniline), respectively, are obtained, compared to that of PANI (216 F/g) at a current density of 200 mA/g between 0.0 and 0.4 V. Moreover, the improved capacitance retention of 73% (12 500 mesh) and 64% (500 mesh) after 500 cycles is obtained for the mass ratios of 1:23

small 2012,
DOI: 10.1002/smll.201102635

small NANO MICRO

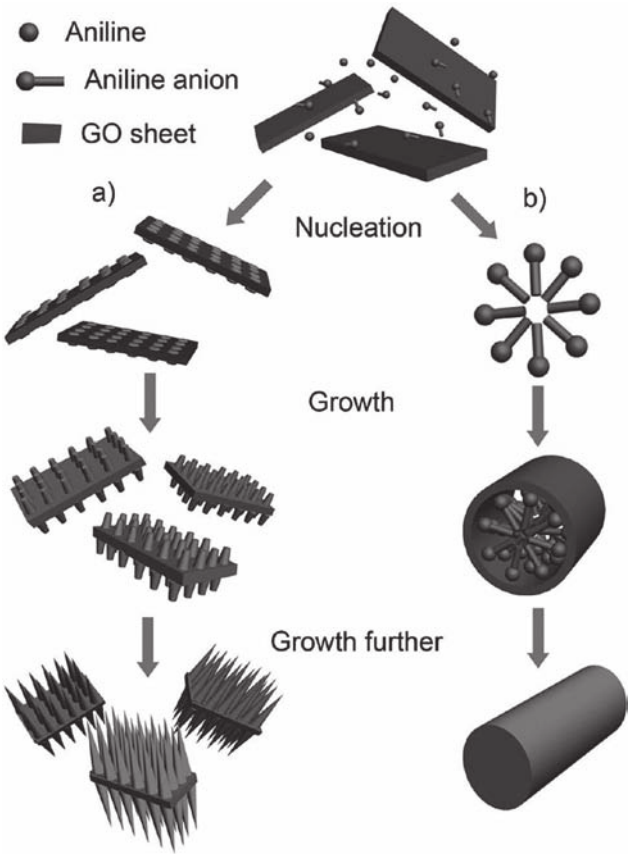

Figure 19. Schematic illustration of nucleation and growth mechanism of PANI nanowires: a) heterogeneous nucleation on GO nanosheets, b) homogeneous nucleation in bulk solution. Reproduced with permission.[136] Copyright 2010, American Chemical Society.

and 1:19, respectively (PANI, 20%). The enhanced specific capacitance and cycling life implies a good synergistic effect between two components.

In another corresponding work, Wei and Han and colleagues[136] investigated a facile method to prepare PANI nanowire arrays vertically aligned on graphene oxide nanosheets as shown in **Figure 19** and **20**. This hierarchical

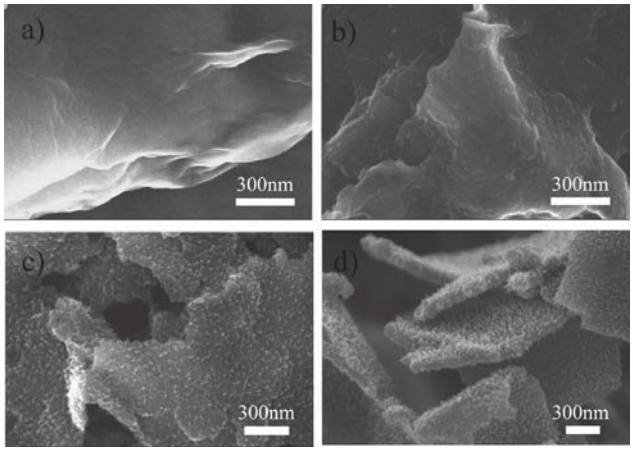

Figure 20. SEM images of PANI–GO samples obtained at different reaction intervals: a) 2.5 h, b) 3 h, c) 8 h, and d) 24 h. Reproduced with permission.[136] Copyright 2010, American Chemical Society.

nanocomposite of PANI nanowire arrays on GO sheets displayed a synergistic effect used as the supercapacitor electrode materials. Not only specific capacitance of the nanocomposite, but also the cycle life of this composite showed better performance than those of the randomly connected PANI nanowires. The specific capacitance of hierarchical PANI–GO was 555 F/g at a discharge current of 0.2 A/g and was still kept as high as 227 F/g even at a discharge current density of 2 A/g. More importantly, after 2000 consecutive cycles, the capacitance retention of hierarchical PANI–GO nanocomposite was maintained at 92% of its initial capacitance, while pristine PANI kept only 74% of its initial capacitance. In general, conducting polymers such as PANI often suffer from a limited long-term stability during cycling because the swelling and shrinking of the polymers may lead to degradation. Thus, the better stability of hierarchical PANI–GO is attributed to the synergistic effect of GO nanosheets and PANI nanowire arrays. GO nanosheets that have unique structural and mechanical properties may restrict the mechanical deformation of PANI nanowires in the redox process, which avoided destroying the electrode material and was benefited to a better stability. Additionally, the vertical nanowire arrays were able to strain relaxation, which made them decrease the breaking during the doping/dedoping process of counterions.[137,138]

4.2. Electrodes Based on (Reduced Graphene)–PANI Composites

Due to the electrochemical instability of GO, GO–PANI composites cannot take advantage of the best potentials of GO, which would be ideal for applications in supercapacitor electrodes; only a small amount of insulating GO has been used in such composites because excess GO would reduce the conductivity of the composite.[134,135] Thus, graphene nanosheets (GNS) are more favorable than GO to be doped into PANI composites. Zhao and co-workers[134] fabricated graphene and PANI nanofiber composites through an in situ polymerization of aniline monomer in the presence of graphene oxide under acidic conditions, which was then followed by the reduction of GO to graphene using hydrazine. Reoxidation and reprotonation of the reduced PANI followed to give the graphene–PANI nanocomposites. They found that the composites that contained 80 wt% of GO showed the highest specific capacitance of 480 F/g at a current density of 0.1 A/g. In addition, when the current density is increased up to 0.5 A/g and even 1 A/g, the specific capacitances still remain at a high level above 200 F/g without a significant decrease upon charge/discharge cycling. While the BET surface areas of all the composites is rather low, i.e., 4.3–20.2 m^2/g, the much higher specific capacitance of this graphene–PANI composite compared with that of pure reduced graphene should be mainly ascribed to the pseudo-capacitance from the PANI nanofibers in the composite. Furthermore, over 70% of the original capacitance was retained after over 1000 cycles, indicating that this electrode material has good cycling stability. This stability is mainly due to the small amount of PANI in the composites.

DOI: 10.1002/smll.201102635

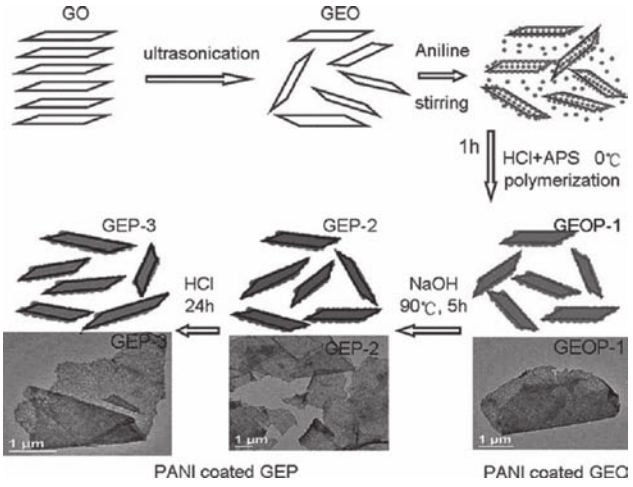

Figure 21. Scheme illustrating the preparation process of the hybrid materials reported by Wang and co-workers. Reproduced with permission.[139] Copyright 2010, Royal Society of Chemistry. In the image, GEO and APS refer to GO and ammonium persulfate, respectively; GEOP-1 represents the composite of GO and APS; GEP-2 represents the product obtained from reducing GEOP-1 and dedoping PANI simultaneously with14.4 mL of 8 M sodium hydroxide at 90 °C for 5 h. GEP-3 represents the product obtained from immersing GEP-2 in 0.2 M HCl for redoping of PANI.

Although the cycling stability of the graphene–PANI composite in the above work is good, their capacitance is still not so satisfying. Thus, Wang and co-workers[139] presented for the first time a simple three-step synthesis method to prepare a graphene–PANI composite as a supercapacitor electrode. As shown in **Figure 21**, this approach was realized by an in situ polymerization/reduction–dedoping/redoping process. It was observed that the reduced graphene sheets are covered by nanostructured PANI granules completely and successfully. They pointed out that this perfect coverage of PANI on graphene fully takes advantage of the large specific area of graphene and could be favorable for the enhancement of the electrochemical properties of the composite materials. The composite material showed better electrochemical performance than both the pure individual components. A high specific capacitance of 1126 F/g was obtained with a retention life of 84% after 1000 cycles for supercapacitors. Such a high retention life for this graphene–PANI composite is mainly due to the change from graphene oxide to graphene in the hybrid material, leading to the improvement of mechanical properties of the composite. In other words, the swelling and shrinkage of PANI during the doping–dedoping processes can be restrained efficiently. Furthermore, the energy density and power density were 34.8 W h/kg and 136 kW/kg, respectively, which were also better than those of the pure component materials. In another report, using graphene-nanosheet support materials to provide active sites for the nucleation of PANI and for excellent electron transfer, Wei and co-workers[140] synthesized a graphene–PANI composite by in situ polymerization. In this case, graphene sheets not only serve as a highly conductive support material, but they also provide a large surface for the well-dispersed deposition of nanoscale PANI particles, resulting in an excellent synergistic effect of graphene and PANI. As a result, the maximum specific capacitance of 1046 F/g is obtained at a scan rate of 1 mV/s for GNS–PANI composite compared to 183 and 115 F/g for GNS and pure PANI, respectively.

Furthermore, it has been confirmed that exfoliated GO precursor can be electrochemically reduced to graphene at cathodic potentials; in the meantime, the aniline monomer can be polymerized at anodic potentials.[141] Accordingly, Huang and Ma[142] developed a new one-step electrochemical synthesis of graphene–PANI composite films in large scale using GO and aniline as the starting materials. Ten cycles of potential scanning at a scan rate of 50 mV/s were used to synthesize the graphene–PANI composite films on an indium tin oxide (ITO) electrode directly with high quality. The specific capacitance value of the fabricated supercapacitor was 640 F/g, and it can maintain its 90% capacitance of the original value after 1000 charge/discharge cycles, indicating good cycling stability. It is suggested that the high specific capacitance and good cycling stability of the supercapacitor might be attributed to the perfect coverage structure of the layered graphene–PANI composite film, the large specific area, and high conductivity.

4.3. Flexible Supercapacitors Prepared from Flexible Graphene–PANI Composite Films

Flexible supercapacitors have many potential applications in various portable electronic devices.[143–145] A freestanding binder-free electrode with favorable mechanical strength and large capacitance is a vital component of a flexible supercapacitor.[146] Free-standing and paper-like graphene-based materials have displayed excellent flexibility, outstanding mechanical strength, and exceptional electrical conductivity, and hence make them potentially suitable for flexible electrochemically active materials, including flexible supercapacitors.[147] Cheng and co-workers[146] aimed to prepare graphene–PANI composite paper (**Figure 22**) as a flexible electrode, by combining the advantages of graphene paper (high conductivity, mechanical strength, and flexibility) and of the PANI conducting polymer (large capacitance). This

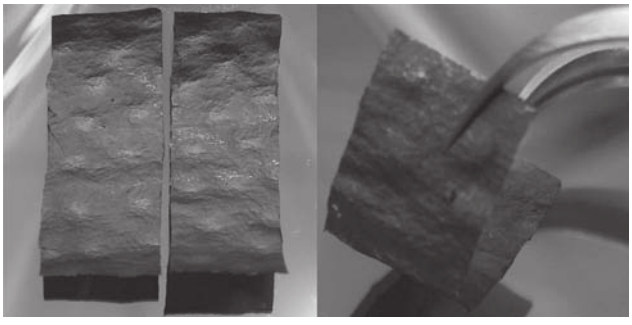

Figure 22. Graphene–PANI composite paper as a flexible electrode. Digital camera images of two freestanding graphene–PANI composite papers (left) and a curved graphene–PANI composite paper (right). Reproduced with permission.[146] Copyright 2009, American Chemical Society.

DOI: 10.1002/smll.201102635

small NANO MICRO

flexible graphene–PANI composite paper was prepared by in situ anodic electropolymerization of aniline monomers into a PANI film on graphene paper. This flexible graphene–PANI composite electrode exhibited important features, such as i) improved electrical conductivity in PANI due to the presence of the graphene paper, ii) homogeneous ion accessibility and high interfacial charge uptake inside the layered structure of the graphene–PANI paper, and iii) a triple supercapacitive storage mechanism (electric double layer charging/discharging and pseudo-capacitive redox reactions of oxygen-containing functional groups of graphene sheet layers and pseudo-capacitive redox reactions of PANI layers). Based on these, this flexible graphene–PANI electrode showed a favorable tensile strength of 12.6 MPa and a stable large electrochemical capacitance of 233 F/g and 135 F/cm^3 for gravimetric and volumetric capacitances, respectively. In another work, Yan and co-workers[147] reported a low-cost technique via simple rapid-mixture polymerization of aniline using graphene papers as substrates to fabricate free-standing, flexible graphene–PANI hybrid papers. Compared to traditional chemical polymerization and electro-polymerization, this rapid-mixture polymerization approach has two advantages: 1) this process is quite simple, and large-area deposition can be realized without the need of costly apparatus and the assistance of heating or cooling, and 2) secondary growth of PANI is limited, resulting in ultrathin PANI coatings with high specific surface area, which were unlikely to destroy the flexibility of the pristine graphene papers. The measured specific capacitance of the graphene–PANI electrode reached as high as 489 F/g. Importantly, after 500 cycles there is still more than 475 F/g remaining at 400 mA/g (above 96% of the original value), illustrating this electrode possesses good cycling stability and lifetime. Therefore, this graphene–PANI hybrid paper is considered to have potential applications in flexible supercapacitors.

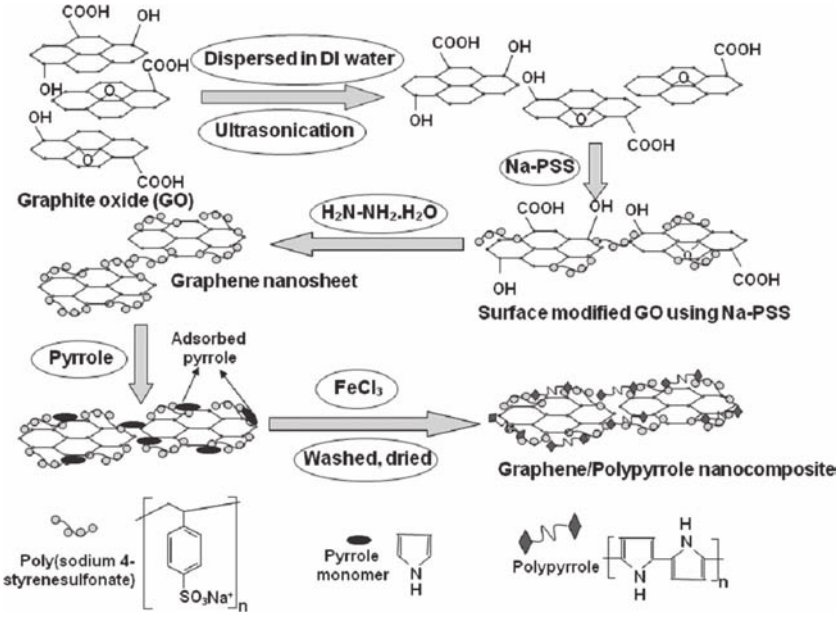

Figure 23. Proposed pathway of the synthesis of graphene–PPy nanocomposites. PSS represents poly(styrene sulfonate). Reproduced with permission.[150] Copyright 2011, IOP Publishing Ltd.

4.4. Electrode Materials Based on Other Graphene–(Conducting Polymer) Composites

Polypyrrole (PPy) has also been used as the conducting polymer for supercapacitor electrodes, owing to its high electrical conduction accompanied by a high stability when exposed to ambient conditions, its ease of synthesis, and its cost -ffectiveness.[148,149] Lee and co-workers[150] established a unique nanoarchitecture involving PPy and graphene nanosheets through in situ polymerization, as displayed in **Figure 23**. In this graphene–PPy composite, graphene nanosheets serve as a support material for the electrochemical utilization of PPy and also provides the path for electron transfer. The specific capacitance value of the nanocomposite achieved 267 F/g at a scan rate of 100 mV/s compared to 137 mV/s for PPy. The authors suggested that the improvement in electrochemical performance of the graphene–PPy nanocomposite, as compared to individual graphene and PPy, was probably due to 1) the oxidation or deoxidation of α- or β-C atoms in the PPy rings, which was facilitated by the presence of graphene nanosheets, 2) the attachment of PPy onto the surface of graphene nanosheets playing a part in reducing diffusion and migration length[151] and thus facilitating the electrochemical utilization of PPy, and 3) the synergistic effect between PPy and graphene nanosheets.[152] The energy density and power density were calculated to be 94.93 W h/kg and 3797.2 W/kg, respectively. Moreover, after 500 cycles, only a 10% decrease in the specific capacitance was noted as compared to the initial value, indicating the improved electrochemical cyclic stability of the nanocomposite.

Zhao and co-workers[153] introduced the conception of electrostatic interactions between negatively charged GO sheets and positively charged surfactant micelles to prepare layered graphene oxide nanostructures with sandwiched conducting polymers as supercapacitor electrodes as shown in **Figure 24**. Two GO–(conducting polymer) composite samples with fibrous and spherical morphologies of the PPy were prepared for comparison. It was found that the morphology of the conducting polymer played a very important role in the electrochemical performance as presented in **Table 1**.

A high specific capacitance of 510 F/g was obtained on the GO–(fibrous PPy) composite, GO–PPy(F), and a high capacitance retention ratio (about 70%) was observed when the current density was increased by 17 times. The GO–(spherical PPy) composite, GO–PPy(S), performed similarly to that of GO–PPy(F) at low current density; however, when the current density increased, GO–PPy(S) performed worse than that of GO–PPy(F) Both the capacitance of GO–PPy(F)

DOI: 10.1002/smll.201102635

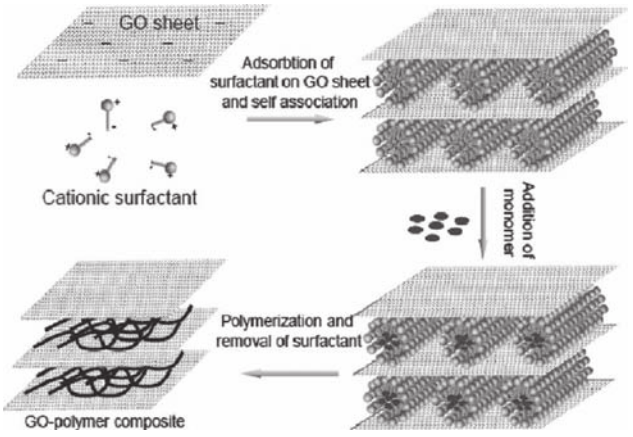

Figure 24. Schematic Illustration of the formation process of the GO–PPy composite. Reproduced with permission.[153] Copyright 2010, American Chemical Society.

and GO–PPy(S) were much better than that of pure PPy. Moreover, over 70% of the original capacitance was retained for the composite electrode GO–PPy(FS) after 1000 cycles, while only 30% was retained for the pure PPy(F) electrode, indicating a much better cycle ability of the composite material than the pure polymer electrode. These attractive results for graphene–PPY composite electrodes are due to 1) the fact that the exfoliated GO sheets dispersed in solution provide a large accessible surface for the attachment of the conducting polymer on both sides; 2) the 3D layered structure enhancing the mechanical strength of the composite and stabilizing the polymers during the charge/discharge process; 3) the GO nanostructure with conducting polymer pillars effectively reducing the dynamic resistance of electrolyte ions; and 4) the readily accessible conducting polymers contributing pseudo-capacitance to the overall energy storage at a significant extent.

Recently, Subramanian, Nair, and co-workers[154] utilized graphene nanolayers, which were synthesized using electrophoretic deposition of graphene, as a scaffold for PPy electropolymerization and created a composite electrode for supercapacitor applications. As depicted in **Figure 25**, the composite electrode structure was highly porous compared with that of the PPy electrode (Figure 25a,b,e,f), and it was believed that this porosity enhances the electrode interaction with the electrolyte. Moreover, PPy nucleated on graphene can utilize the extremely high specific surface area of graphene, and this mode of polymerization is beneficial because it exposes maximum surface sites for Faradic redox reactions of the supercapacitor electrode. As a result, these graphene–PPy composite electrodes exhibited an ultrahigh specific capacitance of 1510 F/g, an area capacitance of 151 mF/cm^2, and a volume capacitance of 151 F/cm^3 at 10 mV/s.

Table 1. Specific gravimetric capacitance of various electrodes at different current densities. GOR represents reduced GO in this table. Reproduced with permission.[153] Copyright 2010, American Chemical Society.

Samples	0.3 A/g	0.5 A/g	1 A/g	2 A/g	3 A/g	5 A/g
GOR	124	98	92			
GO–PPy(F)	510	480	440	456	374	351
PPy(F)	360	250	175	150	120	130
GO–PPy(S)	528	483	364	307	276	255

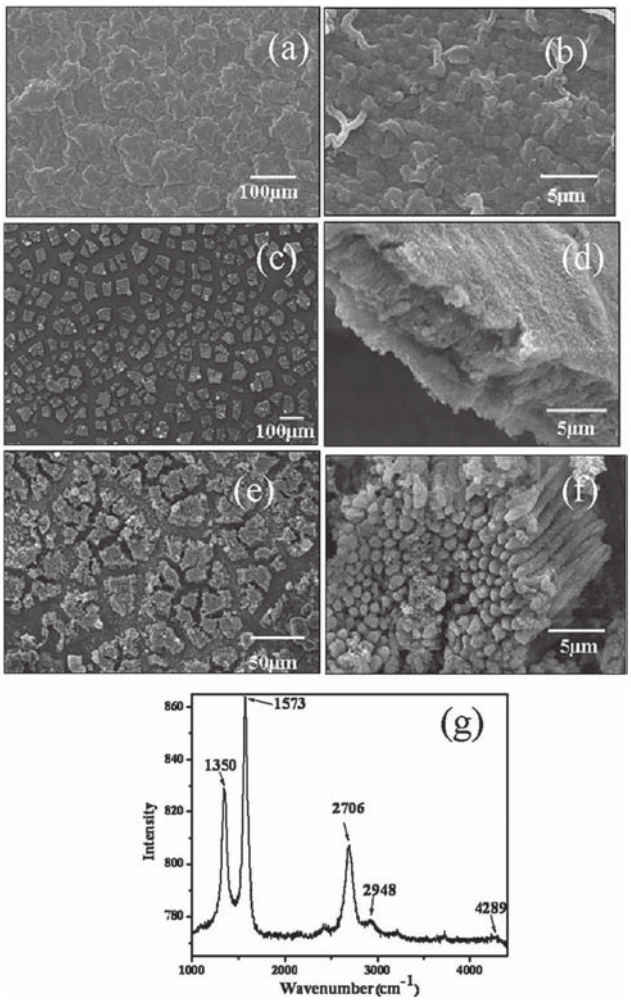

Figure 25. a) SEM image showing electropolymerized pyrrole on Ti; b) magnified image of (a); c) electrophoretic deposition (EPD) of graphene on a Ti plate; d) magnified cross-sectional image of graphene platelets; e) nucleation of polymerization on graphene platelets; f) electropolymerization of pyrrole on graphene platelets; g) Raman spectra of graphene. Reproduced with permission.[154] Copyright 2011, Royal Society of Chemistry.

5. Pseudo-capacitors Based on Graphene–(Metal Oxide) Composites

5.1. Electrode Materials Based on Graphene–MnO_2 Composites

MnO_2 is supposed to be a promising electrode material for applications in supercapacitors and has attracted much attention

DOI: 10.1002/smll.201102635

small NANO MICRO

owing to its environmental compatibility, low cost, and abundant availability on earth.[155] Nevertheless, MnO_2 material prepared from the conventional co-precipitation method has a low specific capacitance due to its low specific surface area.[156] Furthermore, although nanoscale MnO_2 particles possess large surface area and relatively high specific capacitance, the microstructure is easily damaged during electrochemical cycling, resulting in a relatively poor electrochemical stability.[155,157] In addition, the poor electrical conductivity of MnO_2 materials also severely affects their specific capacitance.[158] Given this situation, a promising strategy would be to combine earth-abundant capacitive carbon materials with low-cost pseudo-capacitive metal oxides such as MnO_2, which offers both a cost advantage and potentially a high performance benefiting from both mechanisms of electric double-layer capacitance and pseudo-capacitance.[159]

Zhu and Wang and colleagues[155] first reported a facile and straightforward approach to deposit MnO_2 nanoparticles onto graphene oxide sheets via a simple soft chemical route in water/isopropanol to prepare GO–MnO_2 nanocomposites to be used as supercapacitor electrodes. They supposed the formation mechanism of this novel nanocomposite to be the intercalation and adsorption of manganese ions onto the GO sheets, followed by the nucleation and growth of the crystal species in a double solvent system via dissolution/crystallization and oriented attachment mechanisms, which in turn results in the exfoliation of GO sheets. They confirmed unambiguously that α-MnO_2 nanoneedles had been successfully attached onto the exfoliated GO sheets, as displayed in **Figure 26**. While the specific capacitance for the nano-MnO_2 reached about 211.2 F/g at a current density of 200 mA/g, the specific capacitance value calculated at 150, 200, 500, and 1000 mA/g for this GO–MnO_2 composite was 216.0, 197.2, 141.5, and 111.1 F/g, respectively. Furthermore, they found that the GO–MnO_2 composite electrode retained about 84.1% (165.9 F/g) of initial capacitance after 1000 cycles, while that of the nano-MnO_2 retained only about 69.0% (145.7 F/g). It was considered that the enhanced electrochemical stability for the GO–MnO_2 composite electrode compared to the nano-MnO_2 may be attributable to the different double-layer and pseudo-capacitive contributions; the double-layer process only involves a charge rearrangement, while pseudo-capacitivity is related to a chemical reaction, and the double-layer capacitors have a better electrochemical stability but lower specific capacitance as compared with those of pseudo-capacitors. Consequently, the GO–MnO_2 composite, possessing more double-layer contribution compared to that of nano-MnO_2 due to the presence of GO, have a slightly lower specific capacitance than the latter; however, its electrochemical stability was obviously enhanced.

In another work, Fan and co-workers[158] investigated a quick and easy method to synthesize graphene–MnO_2 composites through the self-limiting deposition of nanoscale MnO_2 on the surface of graphene under microwave irradiation. While the cyclic voltammogram of the carbon–MnO_2 composite usually exhibited a big distortion at a very high scan rate of 500 mV/s in previous reports,[160–162] the cyclic voltammogram for graphene–MnO_2 composite electrodes used in this work still retained a relatively rectangular shape

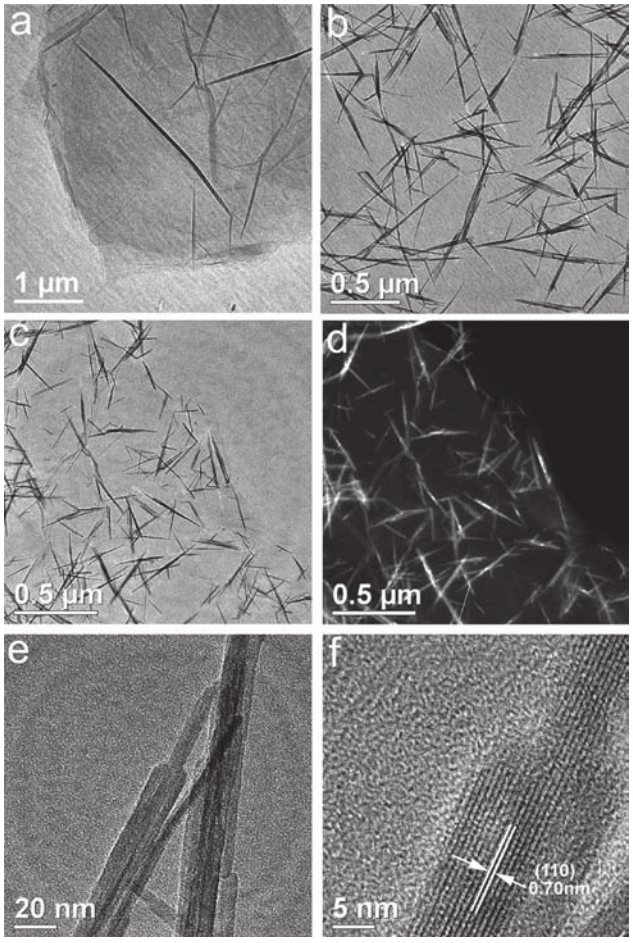

Figure 26. Characterization of GO-MnO_2 nanocomposites. a,b) TEM images of GO and nano-MnO_2. c,d) Bright-field and dark-field images of graphene. e,f) The high-resolution (HR) TEM images of a MnO_2 nanoneedle. Reproduced with permission.[155] Copyright 2010, American Chemical Society.

(**Figure 27**). The graphene–MnO_2 composite containing 78% of MnO_2 exhibited the maximum specific capacitance of 310 F/g at 2 mV/s in 1 M Na_2SO_4 aqueous solution, and the retention ratios were still 88% and 74% at 100 and 500 mV/s respectively. These excellent results for the electrochemical performance of the graphene–MnO_2 composite is considered to be attributed to the following reasons: 1) the MnO_2 nanoparticle coating on the graphene surface can pile up to form pores for ion-buffering reservoirs, improving the diffusion rate of Na^+ within the bulk of the prepared materials; 2) the nanoscale size of the MnO_2 particles (5–10 nm) can greatly reduce the diffusion length over which Na^+ must transfer during the charge/discharge process, improving the electrochemical utilization of MnO_2, and 3) graphene in the composites acted not only as the supports for the deposition of MnO_2 particles but also as a provider of electronic conductive channels, and the excellent interfacial contact between MnO_2 and graphene was of great benefit for fast transportation of electrons throughout the whole electrode matrix. Significantly, the capacitance for the graphene–MnO_2 composite containing 78% of MnO_2 only decreased by 4.6%

DOI: 10.1002/smll.201102635

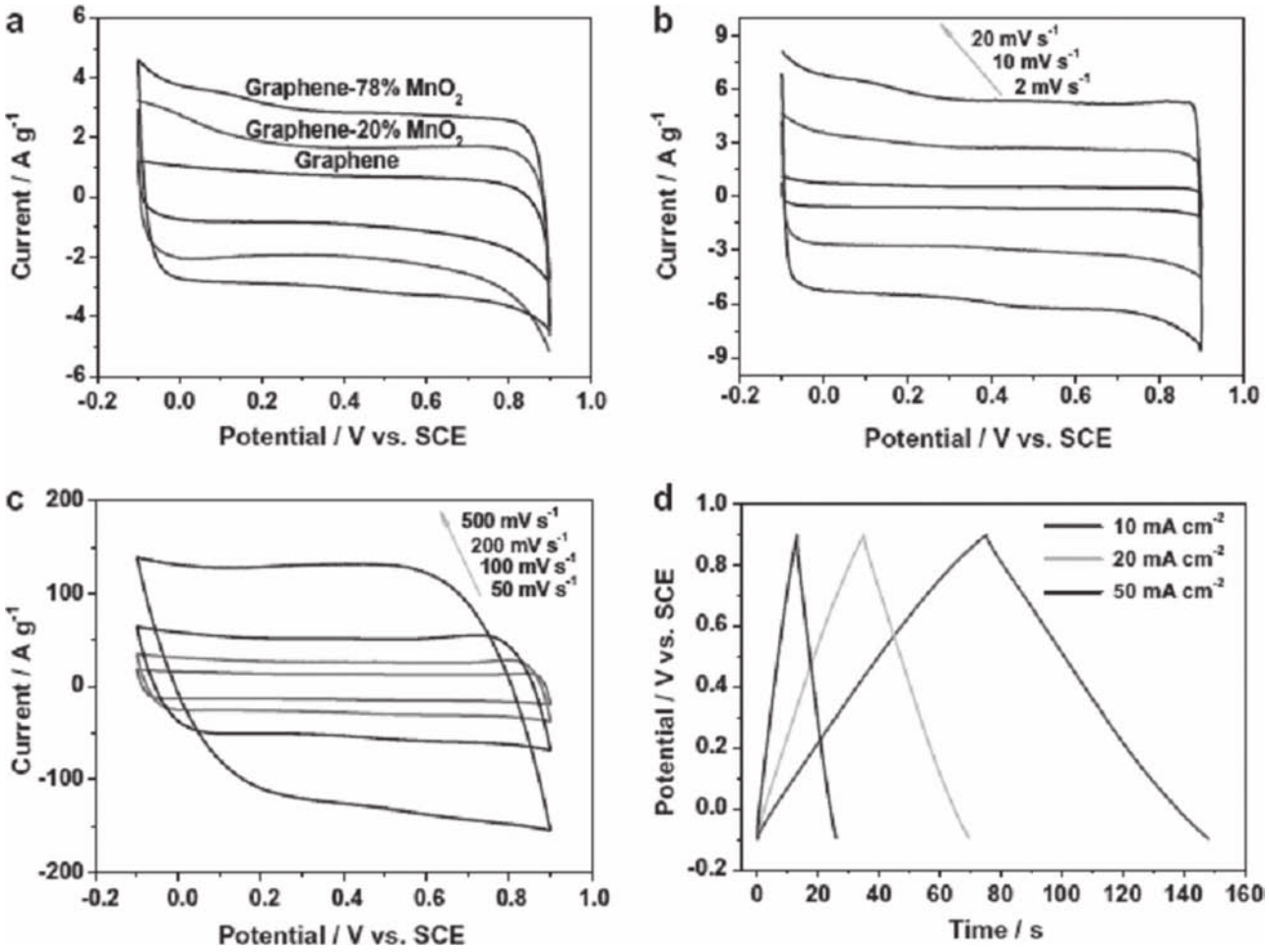

Figure 27. Capacitive properties of graphene–MnO_2 composites. a) CV curves of graphene and graphene–MnO_2 composites at 10 mV/s. b,c) CV curves of graphene–78%MnO_2 composite at different scan rates of 2, 10, 20, 50, 100, 200, and 500 mV/s. d) Galvanostatic charge/discharge curves of graphene–78%MnO_2 composite at current densities of 10, 20, and 50 mA/cm^2 in 1 M Na_2SO_4 solution. Reproduced with permission.[158] Copyright 2010, Elsevier Ltd.

of the initial capacitance after 15 000 cycles at a scan rate of 500 mV/s, indicating the excellent electrochemical stability of such an electrode material.

Zhao and co-workers[163] also developed an intriguing type of graphene–MnO_2 composite use in supercapacitor electrodes. First, they obtained the functionalized graphene by reducing graphene oxide with poly(diallyldimethylammonium chloride) (PDDA), changing the surface charge of reduced graphene oxide from negative to positive. Then, the graphene–MnO_2 composite was prepared by dispersing negatively charged MnO_2 nanosheets on the functionalized reduced graphene sheets via an electrostatic co-precipitation method. The specific capacitance of this composite can reach 188 and 130 F/g at a current density of 0.25 and 4 A/g, respectively, which are much higher values than those of pure functionalized reduced graphene and MnO_2 nanosheets. It was thought that the enhancement in the specific capacitance of the graphene–MnO_2 composite may be due to the contribution of both components. Anchoring of the MnO_2 nanosheets on the functionalized reduced graphene sheets effectively prevent the latter from agglomeration, thus facilitating ion transport in the electrode material, and eventually improving the electric double-layer capacitance. The effective charge transfer in the electrode played an import role in enhancing the specific capacitance and rate capability. For composite sample of functionalized reduced graphene and MnO_2, the face-to-face assembly between the MnO_2 nanosheets and the functionalized reduced graphene sheets, which exhibit good electrical conductivity, results in an intimate interaction of both components, enhancing charge transfer between the two components and leading to rapid redox reactions of the MnO_2 sheets.

In addition to MnO_2, Mn_3O_4 was investigated for use in supercapacitor electrode materials.[164] Wang and co-workers[165] synthesized Mn_3O_4–graphene nanocomposites by mixing a graphene suspension in ethylene glycol with MnO_2 organosol, followed by subsequent ultrasonication processing and heat treatment. While the pure graphene nanosheets have a specific BET surface area of 93.7 m^2/g, it was measured that Mn_3O_4–graphene nanocomposites have a BET area of 1327.3 m^2/g with an increase of more than 14 times, clearly proving the Mn_3O_4 nanoparticles can effectively reduce the stacking of graphene nanosheets. As a result, a high specific capacitance of 256 F/g has been achieved for

small 2012,
DOI: 10.1002/smll.201102635

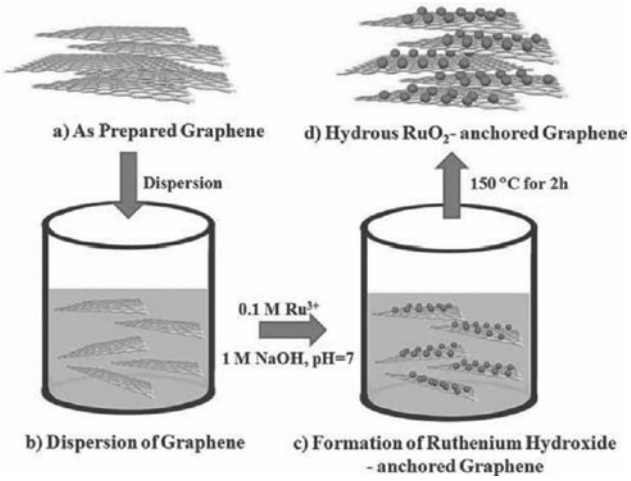

Figure 28. The preparation of ROGSCs by combining a sol–gel method and low-temperature annealing. Reproduced.[169]

Mn_3O_4–graphene nanocomposites, which is almost double that of pure graphene nanosheets.

5.2. Electrode Materials Based on Composites of Graphene and Other Metal Oxides

Despite its high cost, RuO_2 shows great potential for developing supercapacitors with higher energy and power densities than carbon-based EDLCs and polymer-based pseudo-capacitors due to its high capacitance, reversible charge/discharge features, and good electrical conductivity. However, in order to fully utilize the Faradaic and non-Faradaic processes for large-capacity charge storage of RuO_2-based electrode materials, carbon-based materials[166–168] are usually used to prevent the RuO_2 from forming large agglomerates, which may significantly degrade their electrochemical performance as a results of the incomplete reaction of RuO_2 during the electrochemical redox process that starts from the surface of RuO_2 particles and becomes slower as the reaction proceeds, especially for agglomerated large particles.[169,170] Hence, graphene is an excellent choice as the carbon-based substrate materials due to its outstanding properties.

Cheng and co-workers[169] first exploited graphene nanosheets as the substrate material to prepare hydrous ruthenium oxide (RuO_2)–(graphene sheet) composites (ROGSCs) with different loadings of Ru through sol–gel and low-temperature annealing processes (**Figure 28**). It was found that while the as-prepared graphene nanosheets tend to randomly distribut and re-stack, the RuO_2 nanoparticles in the ROGSCs were highly dispersed on the surface of the graphene nanosheets and served as spacers to prevent the graphene sheets from re-stacking. As a result, ROGSCs with 38.3 wt% of Ru (281 m^2/g) had a higher BET specific surface area than that of pure graphene sheets (108 m^2/g) and of pure RuO_2 powder (3.0 m^2/g). The ROGSCs with 38.3 wt% of Ru exhibited a high specific capacitance of ~570 F/g at 1 mV/s, enhanced rate capability, and high energy density (20.1 W h/kg) at low operation rate (100 mA/g) or high power density (10 000 W/kg) at a reasonable energy density (4.3 W h/kg). The total specific capacitance of ROGSCs was higher than the sum of specific capacitances of pure graphene sheets and pure RuO_2 in their relative ratios, indicating a positive synergistic effect of graphene sheets and RuO_2 on the improvement of electrochemical performance. Most importantly, after 1000 cycles at a current density of 1 A/g, 97.9% of the original capacitance was still retained for this ROGSC electrode, which is much higher than the pure RuO_2 electrodes (~42.0%). They believed that this great improvement in electrochemical capacitive performance of ROGSC electrodes was possibly due to the unique particle–sheet structure—which allowed the full utilization of the advantages of both graphene sheets and RuO_2, the greatly decreased interparticle resistance of the electron pathways, the reduced diffusion path, and the facilitated ionic motion during the charge-storage/delivery process.

Dai and co-workers[171] directly grew single-crystalline $Ni(OH)_2$ hexagonal nanoplates on lightly oxided, electrical conducting substrates of graphene nanosheets to prepare advanced electrochemical pseudo-capacitor materials (**Figure 29**). The electrodes that are based on $Ni(OH)_2$–graphene composites showed an intriguing specific

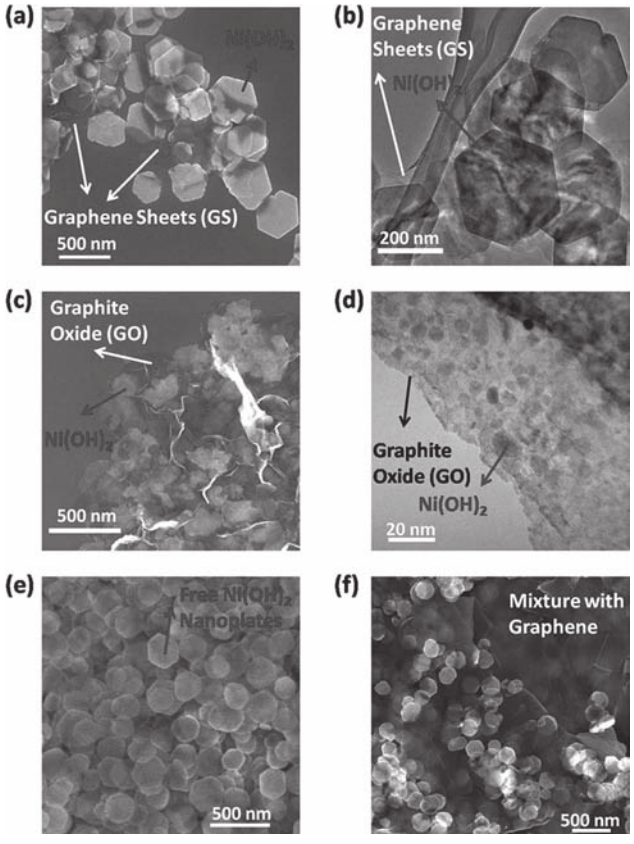

Figure 29. Characterizations of the composite materials. a) SEM image of $Ni(OH)_2$ nanoplates grown on graphene. b) TEM image of $Ni(OH)_2$ nanoplates grown on Graphene. c) SEM image of $Ni(OH)_2$ nanoparticles grown on GO. d) TEM image of $Ni(OH)_2$ nanoparticles grown on GO. e) SEM image of $Ni(OH)_2$ hexagonal nanoplates grown in free solution (without graphene). f) SEM images of simple physical mixture of presynthesized free $Ni(OH)_2$ nanoplates and graphene. Reproduced with permission.[171] Copyright 2010, American Chemical Society.

DOI: 10.1002/smll.201102635

capacitance of ~1335 F/g at a charge and discharge current density of 2.8 A/g. Even at a current density up to 45.7 A/g, this composite electrode still displayed electrochemical characteristics as pseudo-capacitor materials with a specific capacitance of ~952 F/g. The energy density was estimated to be ~37 W h/kg at a power density of ~10 kW/kg in a voltage range of 0.55 V. They concluded that several properties of the composites comprising single-crystalline $Ni(OH)_2$ hexagonal nanoplates and graphene nanosheets contributed to this attractive results. 1) The $Ni(OH)_2$ nanoplates were directly grown and anchored on the graphene sheets through both covalent chemical bonding and van der Waals interactions. This intimate binding afforded facile electron transport between the highly insulating $Ni(OH)_2$ nanoplates and the highly conducting graphene nanosheets, which was key to both the high specific capacitance and rate capability of the $Ni(OH)_2$–graphene materials. With little "dead" volume, most of the $Ni(OH)_2$ nanoplates in the macroscopic ensemble were electrochemically active through the 3D conducting network of graphene nanosheets. Rapid charge transport from the nanoplates to the underlying graphene afforded fast redox reactions at high scan rates and charge and discharge currents. 2) Single-crystalline thin nanoplates showed more favorable electrochemical characteristics over the less crystalline small nanoparticles. Importantly, there was no obvious decrease of the specific capacitance observed after over 2000 cycles of charge/discharge cycling at a high current density of 28.6 A/g, demonstrating excellent cycling stability and long cycle life.

In another work, among the transition metal oxides, Fe_3O_4 is one of the most promising electrode materials due to its low cost and low environmental impact. However, previous work on Fe_3O_4 as supercapacitor electrodes have shown low capacitance values of 60–80 F/g,[172] which is mainly due to its low electrical conductivity; electrical conductivity is needed to enable effective ion diffusion. Yan and co-workers[173] reported a facile technique to fabricate nanocomposites with Fe_3O_4 nanoparticles attached to reduced graphene oxide sheets by a solvothermal process, which combines the growth of Fe_3O_4 nanoparticles and the reduction of graphene oxide sheets in one single step. Then, they further prepared the thin film supercapacitor electrodes by spray-deposition of the Fe_3O_4–(graphene oxide sheet) nanocomposites without insulating binders. This nanocomposite electrode showed much higher specific capacitance than that of either pure reduced graphene or pure Fe_3O_4 nanoparticles due to the much improved electrical conductivity and surface area. The Fe_3O_4–(graphene oxide) nanocomposites with 73.5% Fe_3O_4 nanoparticles displayed 480 F/g at a discharge current density of 5 A/g with the corresponding energy density of 67 W h/kg at a power density of 5506 W/kg, and 843 F/g at a discharge current density of 1 A/g with the corresponding energy density of 124 W h/kg at a power density of 332 W/kg. Strikingly, this composite electrode showed highly stable cycling performance without any decrease in the specific capacitance observed even after 10 000 charge/discharge cycles.

CeO_2 is also one of the attractive candidates for supercapacitor materials because of its environmental friendliness, low cost, and electrochemical redox characteristics.[174] Li and co-workers[175] reported the fabrication of CeO_2 nanoparticles/graphene nanocomposite by depositing CeO_2 nanoparticles onto 3D graphene material, and further investigated its supercapacitor performance. Although not too high, the specific capacitance of this CeO_2–graphene nanocomposite (~208 F/g) was still much better than that of the pure graphene nanosheets (~78 F/g). This indicated that the combination of CeO_2 with graphene indeed produced a synergistic effect to remarkably boost its high capacitance. This effect may be associated with the fact that 1) the CeO_2 modification increases graphene hydrophilicity significantly increasing its applicability for porous electrodes, and 2) that the conductive graphene enhances the charge transfer rate of CeO_2 for higher pseudo-capacitance. In addition, the capacitance of active materials drops insignificantly after 1000 cycles at a current density of 1 A/g, which proved that the cycle life of graphene–CeO_2 electrodes was excellent.

Furthermore, Wang, Zhu, and co-workers[176] reported a facile soft chemical approach to fabricate graphene–$Co(OH)_2$ nanocomposites in a water–isopropanol system. They utilized Na_2S as a precursor, which enabled the deposition of Co^{2+} and the deoxygenation of GO at the same time. Remarkably, the electrochemical specific capacitance of the graphene–$Co(OH)_2$ nanocomposite reaches a value as high as 972.5 F/g at the current density of 500 mA/g, leading to a significant improvement in relation to each individual counterpart (137.6 and 726.1 F/g for graphene and $Co(OH)_2$, respectively). The decoration of graphene sheets with $Co(OH)_2$ nanocrystals effectively inhibit aggregation, which resulted in a relatively higher utilization of $Co(OH)_2$ and therefore increased electrochemical performance of the nanocomposite.

Cobalt oxide has also been reported to be a promising electrode material for supercapacitors because of its relatively low cost, high redox activity, high theoretical specific capacitance (~3560 F/g), and good reversibility.[177] Fan and co-workers[178] employed the microwave-assisted method to synthesize the (graphene nanosheet)–Co_3O_4 composites for use as supercapacitor electrodes. The maximum specific capacitance of 243.2 F/g is obtained at 10 mV/s in 6 M KOH aqueous solution for the graphene–Co_3O_4 composite, much higher than that of pure GNS (169.3 F/g). Furthermore, the specific capacitance of the graphene–Co_3O_4 composite is still 174.9 F/g at a scan rate of 100 mV/s. They concluded that the improvement is probably attributed to the unique structure of the composite. Firstly, the well-dispersed nanoscale Co_3O_4 particles on graphene could not only effectively inhibit the stacking/agglomerating of graphene sheets, resulting in high double-layer capacitance, but it also ensured that the Co_3O_4 were more accessible for the necessary electrochemical reactions. Secondly, graphene sheets provided a highly conductive network for electron transport during the charge and discharge processes. Finally, the excellent interfacial contact and increased contact area between Co_3O_4 and graphene sheets can significantly improve the accessibility of this composite to the electrolyte ions and shorten the ion diffusion and migration pathways. Furthermore, this composite electrode also showed long-term cycle stability, and only a 4.4% decrease of the initial capacitance was observed after 2000 cycles at a scan rate of 200 mV/s.

DOI: 10.1002/smll.201102635

small NANO MICRO

Hu and co-workers[179] synthesized composites of ZnO and reduced graphene oxide using a two-step method in which KOH reacts with $Zn(NO_3)_2$ in the aqueous dispersions of GO to form a $Zn(OH)_2$–(graphene oxide) precursor, followed by thermal treatment in air. This composite, containing only 6.7% of reduced graphene oxide, consisted almost entirely of reduced graphene oxide sheets coated by ZnO, and it achieved a specific capacitance as high as 308 F/g at a specific current of 1 A/g, which is much higher when compared with the individual values of the two components, 135 and 157 F/g for pure ZnO and bare reduced graphene oxide, respectively. Importantly, even at the high specific current of 4 A/g, a specific capacitance of 180 F/g is achieved, implying that the composite of this ratio has a relatively good rate capability at a large specific current density. A mere 6.5% decay in the available capacitance was observed after 1500 cycles for this composite electrode, indicating good cycling stability.

6. Graphene-Based Asymmetric Supercapacitors

While great efforts have been made to investigate the electrochemical capacitors with high power density (larger than 10 kW/kg) due to their faster charge and discharge processes than those of batteries,[34] electrochemical capacitors usually suffer from a lower energy density (normally ≤10 W h/kg) than batteries.[180] Thus, in order to resolve this problem, asymmetric supercapacitors have been extensively explored by combining Faradic electrode (as energy source) and the capacitive electrode (as power source) to increase the operation voltage, which leads to an obvious improvement of the energy density of high-power ECs (electrochemical capacitors). so that it approaches that of batteries.[181–185] The key issue for achieving high energy and power densities in asymmetric supercapacitors is the development of appropriate electrode materials.[186] Usually, carbon-based materials with high surface area, which store charges electrostatically via reversible ion absorption at the electrode/electrolyte interface, can be utilized as capacitive electrodes.[37,187] In contrast, transition metal oxides such as RuO_2, Fe_3O_4, NiO, and MnO_2, and conducting redox polymers such as PANI, PPy, and poly(thiophene) (PTH), which use fast and reversible redox reactions at the surface of the electroactive materials for charge storage, are utilized as pseudo-capacitor electrodes.[188–191]

Therefore, for the purpose of achieving high energy and power densities, Cheng, Ren, and co-workers[186] developed a high-voltage asymmetric supercapacitor with graphene as the negative electrode and a MnO_2–graphene composite as the positive electrode in aqueous Na_2SO_4 solution electrolyte. The MnO_2–graphene composite was prepared through solution-phase assembly of graphene sheets and α-MnO_2 nanowires. Graphene is a good candidate for the capacitive electrode since it can provide a large accessible surface area for fast transport of hydrate ions to achieve high double-layer capacitance in aqueous electrolytes.[75,89] Moreover, the superior electrical conductivity of graphene makes a nanostructured MnO_2–graphene composite, which is promising for use as Faradic electrodes in asymmetric ECs. More importantly, the presence of nanostructured MnO_2 is able to efficiently prevent the aggregation of graphene sheets caused by van der Waals interactions, consequently leading to an increase in the available electrochemical active surface area and a suitable porous structure for energy storage. As a result, this aqueous-electrolyte-based asymmetric ECs can be cycled reversibly in the high-voltage region of 0–2.0 V and exhibited a superior energy density of 30.4 W h/kg, which is much higher than those of symmetric ECs based on graphene//graphene (2.8 W h/kg) and MGC//MGC (5.2 W h/kg; MGC = modified glassy carbon). Moreover, they present a high power density (5000 W/kg at 7.0 W h/kg) and acceptable cycling performance of ~79% retention after 1000 cycles.

In another work, Bao and Cui and co-workers[159] demonstrated a novel structure of a supercapacitor electrode based on graphene–MnO_2–textiles where solution-exfoliated graphene nanosheets were conformably coated on porous textile fibers, serving as conductive 3D frameworks for subsequently controlled electrodeposition of MnO_2 nanomaterials (**Figure 30**). Such a 3D porous networks not only permitted large loading of active electrode materials but also facilitated easy access of electrolytes to the electrodes. The hybrid graphene–MnO_2-based textile could yield high-capacitance performance with specific capacitance values up to 315 F/g at a scan rate of 2 mV/s. Several unique characteristics of these graphene–MnO_2 nanostructured textiles made them promising candidates for high-performance supercapacitor electrode materials. 1) The 3D porous microstructures of the polyester textiles allowed uniform coating of graphene nanosheets and subsequent loading of MnO_2, facilitating access of electrolyte ions to electrode surfaces. 2) The graphene nanosheet coatings served as high-surface-area, conductive paths for the deposition of MnO_2, providing excellent interfacial contact between MnO_2 and graphene for fast electron transport; and 3) the nanoflower architectures of electrodeposited MnO_2 offered a large electrochemically active surface area for charge transfer and reduced ion diffusion length during the charge/discharge process. Based on these results, the authors further exploited the graphene–MnO_2 textile as the positive electrodes and single-walled carbon nanotubes (SWNT)-textiles as the negative electrodes to assemble hybrid supercapacitors in 0.5 M Na_2SO_4 aqueous electrolytes. The maximum energy density of 12.5 W h/kg and the highest power density of 110 kW/kg are achieved for these asymmetric supercapacitors at an operation voltage of 1.5 V. Importantly, the cycling test of the asymmetric supercapacitors cells shows ~95% capacitance retention over 5000 cycles at a high current density of 2.2 A/g.

Tan, Qin, and co-workers[192] successfully fabricated binderless supercapacitors using electroactivated graphene paper as negative electrodes and graphene films coated with MnO_2 nanoflowers as positive electrode, as shown in **Figure 31**. The electroactivated graphene film showed a high specific capacitance of 245 F/g, and the MnO_2-coated graphene film displayed high specific capacitance of 328 F/g. Moreover, the power density of the asymmetric supercapacitor reached 25.8 kW/kg and the energy density reached 11.4 W h/kg. The

DOI: 10.1002/smll.201102635

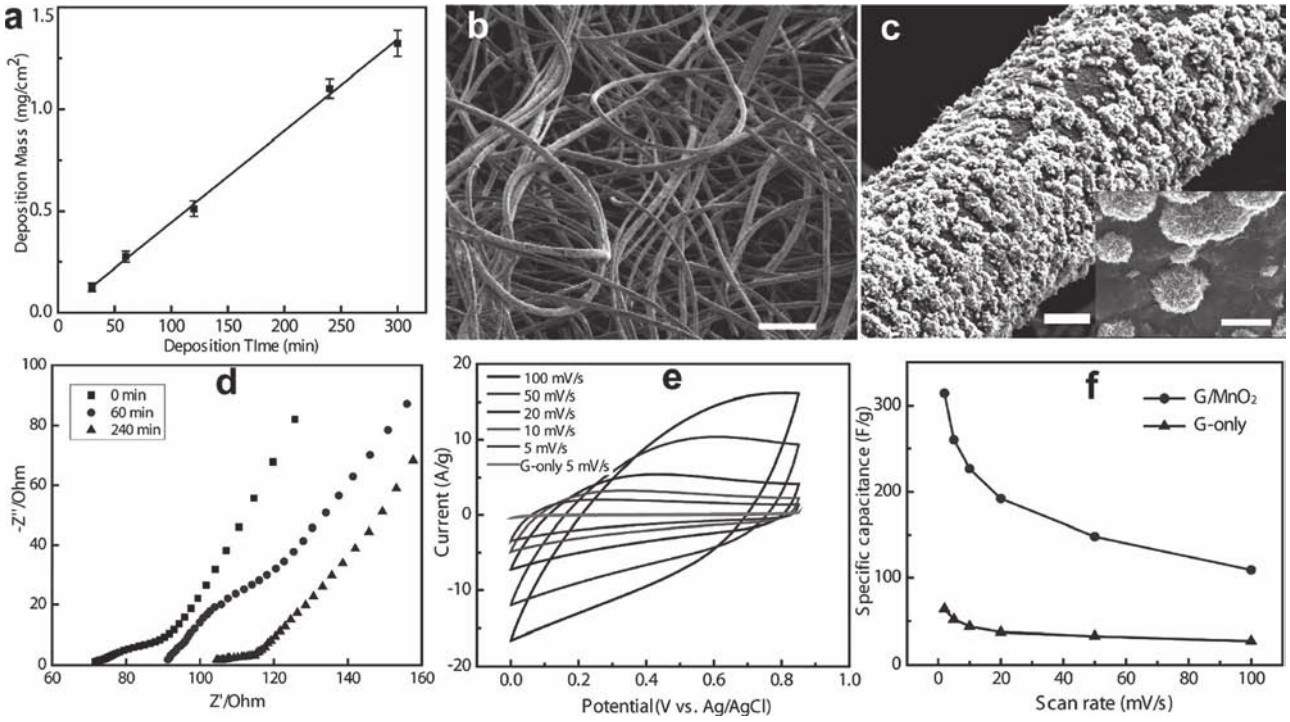

Figure 30. Supercapacitors based on graphene–MnO_2–textiles. a) MnO_2 electrodeposition curve. b) SEM image of a sheet of graphene-coated textile. c) SEM image of a typical microfiber with a coating of MnO_2 nanostructures. d) Impedance of graphene–MnO_2–textiles with different MnO_2 deposition time. e) Cyclic voltammograms for graphene(G)–MnO_2–textile electrode at different scan rates. f) Comparison of specific capacitance values between graphene–MnO_2–textile and a graphene–nanosheet-only textile at different scan rates. Reproduced with permission.[159] Copyright 2011, American Chemical Society.

activation process for the graphene film can let the ions in the electrolyte intercalate into the spaces between the graphene layers and produce more surface area for the ions to access, thus improving the specific capacitance of the graphene film. The outstanding properties of the MnO_2-coated graphene film are attributed to the high accessible specific surface area and high efficiency of electrolyte ion absorption. Graphene sheets with either individual single-layered sheets or few-layered graphite can offer an ideal structure for ion absorption of MnO_2.

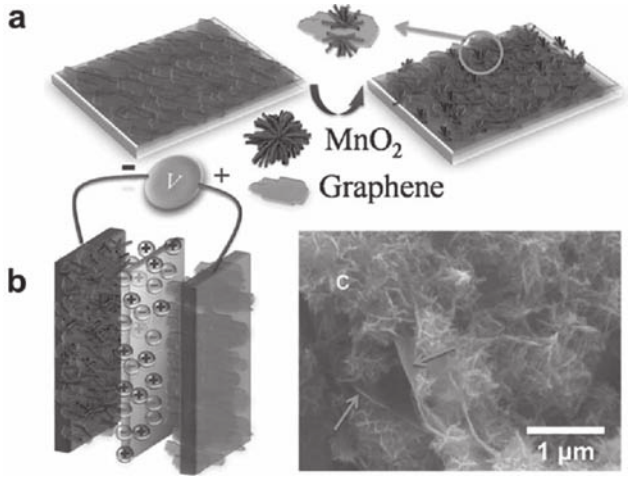

Figure 31. Schemes illustrating coating of graphene with MnO_2 nanoflowers. a) Schematic of the graphene electrode and the MnO_2-coated graphene electrode. b) Schematic of asymmetric supercapacitor with graphene as anode and MnO_2-coated graphene as cathode. c) SEM image of the MnO_2-coated graphene, where the graphene nanosheets are indicated by arrows. Reproduced with permission.[192] Copyright 2011, Elsevier Ltd.

A novel kind of asymmetric supercapacitor using a graphene–MnO_2 composite as the positive electrode and activated carbon nanofibers (ACN) as the negative electrode in a neutral aqueous Na_2SO_4 electrolyte was also developed by Wei and co-workers.[193] The graphene–MnO_2 composites were synthesized by a self-limiting deposition of nanoscale MnO_2 on the surface of graphene under microwave irradiation.[158] ACN derived from rod-shaped PANI was synthesized by carbonization and subsequent activation with KOH.[194] This optimized asymmetric supercapacitor can be cycled reversibly between 0 and 1.8 V in 1 M Na_2SO_4 solution. A maximum specific capacitance of 113.5 F/g with a measured energy density of 51.1 W h/kg was thus obtained. At the same time, the supercapacitor device exhibited superior long cycle life along with ~97% specific capacitance retained after 1000 cycles. These superior electrochemical performances are mainly due to the high capacitances and excellent rate performances of the graphene–MnO_2 composite nd ACN, as well as the synergistic effects of the two electrodes for the asymmetric supercapacitors.

Dai and co-workers[195] grew $Ni(OH)_2$ nanoplates and RuO_2 nanoparticles on high-quality graphene sheets to maximize the specific capacitances of these materials. Subsequently, they paired up a $Ni(OH)_2$–graphene electrode with

DOI: 10.1002/smll.201102635

small NANO MICRO

a RuO_2–graphene electrode to afford a high-performance asymmetrical supercapacitor with high energy and power densities operating in aqueous solutions at a voltage of ~1.5 V. The specific capacitance for this asymmetric supercapacitor was ~160 F/g at a current density of 0.5 A/g, and at a high current density of 20 A/g, a useful capacitance of ~97 F/g was measured. Furthermore, the asymmetrical supercapacitor also exhibited good cycling stability with a stable capacitance (~92% of the original capacitance) after ~5000 cycles of charging and discharging at a current density of 10 A/g. Importantly, the asymmetrical supercapacitor showed a high energy density of ~48 W h/kg at a power density of ~0.23 kW/kg, and a high power density of ~21 kW/kg at an energy density of ~14 W h/kg, which are significantly higher than that of the symmetrical RuO_2–RuO_2 supercapacitors. These high performances were considered to be mainly attributed to the advanced hybrid electrode materials and their unique pairing.

7. Conclusion and Outlook

Based on our journey for graphene-based materials for supercapacitors, it can be concluded that although most of the research has only been at a peak since 2008, graphene-based materials are indeed very fascinating materials with great potential in the active field of supercapacitors. In theory, graphene has been considered to be the ideal supercapacitor electrode material due to its extremely large surface area, extraordinarily high electrical conductivity,and strong mechanical strength. In practice however, massive efforts are still needed to turn this promising material into a real practical material. The most essential problem lies in how to prepare large-scale and high-quality graphene-based materials in a cost-effective way. Until now, two methods—the chemical exfoliation of graphite into graphene oxide followed by controllable reduction to make reduced graphene materials or the in situ reaction (with transition metal oxides or conducting polymer precursor) to fabricate graphene-based composite materials—have been widely investigated and deemed as the most promising for producing supercapacitor electrodes. Another challenge is that graphene material is easy to re-stack, which causes the decline of its physical properties and processability. Some efficient methods, including the functionalization of graphene or the addition of spacers between the graphene layers, have been presented to solve this problem.

For the graphene-based EDLC applications, the conductivity and large SSA of graphene are two crucial factors for making high-performance supercapacitors. A series of effective routes, such as low-temperature thermal exfoliation, solvothermal processing, microwave heating, introduction of spacer materials, and activation, have been utilized to reduce GO, to restore the conductivity and intrinsic SSA of graphene as much as possible, and to tune for the proper spacing size needed for the intercalating of ions. However, achieving a state with individual graphene layers and fully utilizing the SSA of perfect graphene is still a challenge, and thus future efforts are still needed for the development of more efficient fabrication techniques in order to reach enhanced performance.

As for graphene-based composite electrodes in the pseudo-supercapacitor applications, it has been demonstrated that the improvement of the electrochemical performance of the graphene-based composite electrodes is mainly attributed to the following reasons. 1) Graphene in composites can act as supports for the deposition of active component at the nanoscale, and thus can increase the SSA of the active components. 2) Graphene can also provide the electronic conductive channels, and the excellent interfacial contact between the active component and graphene is of great benefit to the fast transportation of electrons throughout the entire electrode matrix. 3) Graphene nanosheets have unique structural and mechanical properties, which can restrict the mechanical deformation of the active component during the redox process; this avoids destruction of the electrode material and leads to better stability.

Graphene-based materials have great potential for application in supercapacitors and other green energy devices. The key issue is to fully utilize graphene's excellent intrinsical properties, especially its high surface area and high conductivity, and to improve the synergistic effect of the graphene substrate with the other active components. The design and synthesis of new nanostructures and architectures based on graphene will be be an important task in the future.

Acknowledgements

The authors gratefully acknowledge financial support from MOST (Grants 2012CB933401, 2011CB932602 and 2011DFB50300), NSFC (Grants 50933003, 50902073 and 50903044).

[1] A. K. Geim, K. S. Novoselov, *Nat. Mater.* **2007**, *6*, 183.
[2] J. C. Meyer, A. K. Geim, M. I. Katsnelson, K. S. Novoselov, T. J. Booth, S. Roth, *Nature* **2007**, *446*, 60.
[3] R. R. Nair, P. Blake, A. N. Grigorenko, K. S. Novoselov, T. J. Booth, T. Stauber, N. M. R. Peres, A. K. Geim, *Science* **2008**, *320*, 1308.
[4] T. J. Booth, P. Blake, R. R. Nair, D. Jiang, E. W. Hill, U. Bangert, A. Bleloch, M. Gass, K. S. Novoselov, M. I. Katsnelson, A. K. Geim, *Nano Lett.* **2008**, *8*, 2442.
[5] C. Lee, X. D. Wei, J. W. Kysar, J. Hone, *Science* **2008**, *321*, 385.
[6] P. Avouris, Z. H. Chen, V. Perebeinos, *Nat. Nanotechnol.* **2007**, *2*, 605.
[7] K. S. Novoselov, A. K. Geim, S. V. Morozov, D. Jiang, Y. Zhang, S. V. Dubonos, I. V. Grigorieva, A. A. Firsov, *Science* **2004**, *306*, 666.
[8] A. A. Balandin, S. Ghosh, W. Z. Bao, I. Calizo, D. Teweldebrhan, F. Miao, C. N. Lau, *Nano Lett.* **2008**, *8*, 902.
[9] J. L. Xia, F. Chen, J. H. Li, N. J. Tao, *Nat. Nanotechnol.* **2009**, *4*, 505.
[10] J. J. Liang, Y. Huang, L. Zhang, Y. Wang, Y. F. Ma, T. Y. Guo, Y. Chen, *Adv. Funct. Mater.* **2009**, *19*, 2297.
[11] S. Stankovich, D. A. Dikin, G. H. B. Dommett, K. M. Kohlhaas, E. J. Zimney, E. A. Stach, R. D. Piner, S. T. Nguyen, R. S. Ruoff, *Nature* **2006**, *442*, 282.
[12] X. Huang, X. Y. Qi, F. Boey, H. Zhang, *Chem. Soc. Rev.* **2012**, *41*, 666.

DOI: 10.1002/smll.201102635

[13] H. A. Becerril, J. Mao, Z. Liu, R. M. Stoltenberg, Z. Bao, Y. Chen, *ACS Nano* **2008**, *2*, 463.
[14] K. S. Kim, Y. Zhao, H. Jang, S. Y. Lee, J. M. Kim, K. S. Kim, J. H. Ahn, P. Kim, J. Y. Choi, B. H. Hong, *Nature* **2009**, *457*, 706.
[15] X. Li, G. Zhang, X. Bai, X. Sun, X. Wang, E. Wang, H. Dai, *Nat. Nanotechnol.* **2008**, *3*, 538.
[16] Q. Y. He, S. X. Wu, S. Gao, X. H. Cao, Z. Y. Yin, H. Li, P. Chen, H. Zhang, *ACS Nano* **2010**, *4*, 5263.
[17] F. Schedin, A. K. Geim, S. V. Morozov, E. W. Hill, P. Blake, M. I. Katsnelson, K. S. Novoselov, *Nat. Mater.* **2007**, *6*, 652.
[18] Q. Y. He, H. G. Sudibya, Z. Y. Yin, S. X. Wu, H. Li, F. Boey, W. Huang, P. Chen, H. Zhang, *ACS Nano* **2010**, *4*, 3201.
[19] J. J. Liang, Y. F. Xu, Y. Huang, L. Zhang, Y. Wang, Y. F. Ma, F. F. Li, T. Y. Guo, Y. S. Chen, *J. Phys. Chem. C* **2009**, *113*, 9921.
[20] S. Park, J. An, J. W. Suk, R. S. Ruoff, *Small* **2010**, *6*, 210.
[21] X. J. Xie, L. T. Qu, C. Zhou, Y. Li, J. Zhu, H. Bai, G. Q. Shi, L. M. Dai, *ACS Nano* **2010**, *4*, 6050.
[22] J. J. Liang, Y. Huang, J. Oh, M. Kozlov, D. Sui, S. L. Fang, R. H. Baughman, Y. F. Ma, Y. S. Chen, *Adv. Funct. Mater.* **2011**, *21*, 3778.
[23] A. Das, S. Pisana, B. Chakraborty, S. Piscanec, S. K. Saha, U. V. Waghmare, K. S. Novoselov, H. R. Krishnamurthy, A. K. Geim, A. C. Ferrari, A. K. Sood, *Nat. Nanotechnol.* **2008**, *3*, 210.
[24] B. Li, X. H. Cao, H. G. Ong, J. W. Cheah, X. Z. Zhou, Z. Y. Yin, H. Li, J. L. Wang, F. Boey, W. Huang, H. Zhang, *Adv. Mater.* **2010**, *22*, 3058.
[25] D. A. C. Brownson, D. K. Kampouris, C. E. Banks, *J. Power Sources* **2011**, *196*, 4873.
[26] M. Pumera, *Chem. Soc. Rev.* **2010**, *39*, 4146.
[27] M. Pumera, *Energy Environ. Sci.* **2011**, *4*, 668.
[28] Y. Sun, Q. Wu, G. Shi, *Energy Environ. Sci.* **2011**, *4*, 1113.
[29] A. S Arico, P. Bruce, B. Scrosati, J. M. Tarascon, W. Van Schalkwijk, *Nat. Mater.* **2005**, *4*, 366.
[30] A. G. Pandolfo, A. F. Hollenkamp, *J. Power Sources* **2006**, *157*, 11.
[31] M. Winter, R. J. Brodd, *Chem. Rev.* **2004**, *104*, 4245.
[32] A. Burke, *J. Power Sources* **2000**, *91*, 37.
[33] J. R. Miller, P. Simon, *Science* **2008**, *321*, 651.
[34] P. Simon, Y. Gogotsi, *Nat. Mater.* **2008**, *7*, 845.
[35] S. R. C. Vivekchand, C. S. Rout, K. S. Subrahmanyam, A. Govindaraj, C. N. R. Rao, *J. Chem. Sci.* **2008**, *120*, 9.
[36] R. Kotz, M. Carlen, *Electrochim. Acta* **2000**, *45*, 2483.
[37] B. E. Conway, *Electrochemical Supercapacitors. Scientific Fundamentals and Technological Applications*, Kluwer Academic, Plenum, New York **1999**.
[38] M. D. Stoller, S. J. Park, Y. W. Zhu, J. H. An, R. S. Ruoff, *Nano Lett.* **2008**, *8*, 3498.
[39] G. A. Snook, P. Kao, A. S. Best, *J. Power Sources* **2011**, *196*, 1.
[40] L. L. Zhang, X. S. Zhao, *Chem. Soc. Rev.* **2009**, *38*, 2520.
[41] E. Frackowiak, F. Beguin, *Carbon* **2001**, *39*, 937.
[42] D. Y. Qu, H. Shi, *J. Power Sources* **1998**, *74*, 99.
[43] S. T. Mayer, R. W. Pekala, J. L. Kaschmitter, *J. Electrochem. Soc.* **1993**, *140*, 446.
[44] C. M. Niu, E. K. Sichel, R. Hoch, D. Moy, H. Tennent, *Appl. Phys. Lett.* **1997**, *70*, 1480.
[45] E. Frackowiak, K. Metenier, V. Bertagna, F. Beguin, *Appl. Phys. Lett.* **2000**, *77*, 2421.
[46] K. H. An, W. S. Kim, Y. S. Park, Y. C. Choi, S. M. Lee, D. C. Chung, D. J. Bae, S. C. Lim, Y. H. Lee, *Adv. Mater.* **2001**, *13*, 497.
[47] C. S. Du, J. Yeh, N. Pan, *Nanotechnology* **2005**, *16*, 350.
[48] S. Yoon, J. W. Lee, T. Hyeon, S. M. Oh, *J. Electrochem. Soc.* **2000**, *147*, 2507.
[49] J. Chmiola, G. Yushin, Y. Gogotsi, C. Portet, P. Simon, P. L. Taberna, *Science* **2006**, *313*, 1760.
[50] M. M. Shaijumon, F. S. Ou, L. Ci, P. M. Ajayan, *Chem. Commun.* **2008**, 2373.
[51] L. Diederich, E. Barborini, P. Piseri, A. Podesta, P. Milani, A. Schneuwly, R. Gallay, *Appl. Phys. Lett.* **1999**, *75*, 2662.
[52] C. G. Liu, M. Liu, F. Li, H. M. Cheng, *Appl. Phys. Lett.* **2008**, *92*, 143108.
[53] K. H. An, W. S. Kim, Y. S. Park, J. M. Moon, D. J. Bae, S. C. Lim, Y.S. Lee, Y. H. Lee, *Adv. Funct. Mater.* **2001**, *11*, 387.
[54] W. Deng, X. Ji, Q. Chen, C. E. Banks, *Rsc Adv.* **2011**, *1*, 1171.
[55] C. D. Lokhande, D. P. Dubal, O. S. Joo, *Curr. Appl. Phys.* **2011**, *11*, 255.
[56] C. Peng, S. Zhang, D. Jewell, G. Z. Chen, *Prog. Nat. Sci. Mater. Int.* **2008**, *18*, 777.
[57] Q. Yu, J. Lian, S. Siriponglert, H. Li, Y. P. Chen, S. S. Pei, *Appl. Phys. Lett.* **2008**, *93*, 113103.
[58] Y. Zhu, S. Murali, W. Cai, X. Li, J. W. Suk, J. R. Potts, R. S. Ruoff, *Adv. Mater.* **2010**, *22*, 3906.
[59] X. Li, W. Cai, J. An, S. Kim, J. Nah, D. Yang, R. Piner, A. Velamakanni, I. Jung, E. Tutuc, S. K. Banerjee, L. Colombo, E. S. Ruoff, *Science* **2009**, *324*, 1312.
[60] Y. B. Zhang, J. P. Small, W. V. Pontius, P. Kim, *Appl. Phys. Lett.* **2005**, *86*, 073104.
[61] Y. Hernandez, V. Nicolosi, M. Lotya, F. M. Blighe, Z. Sun, S. De, I. T. McGovern, B. Holland, M. Byrne, Y. K. Gun'ko, J. J. Boland, P. Niraj, G. Duesberg, S. Krishnamurthy, R. Goodhue, J. Hutchison, V. Scardaci, A. C. Ferrari, J. N. Coleman, *Nat. Nanotechnol.* **2008**, *3*, 563.
[62] A. Dato, V. Radmilovic, Z. Lee, J. Phillips, M. Frenklach, *Nano Lett.* **2008**, *8*, 2012.
[63] Y. Wu, B. Wang, Y. Ma, Y. Huang, N. Li, F. Zhang, Y. Chen, *Nano Res.* **2010**, *3*, 661.
[64] B. C. Brodie, *Ann. Chim. Phys.* **1860**, *59*, 466.
[65] L. Staudenmaier, *Ber. Deut. Chem. Ges.* **1898**, *31*, 1481.
[66] W. S. O. Hummers, *J. Am. Chem. Soc.* **1958**, *80*, 1339.
[67] M. Hirata, T. Gotou, S. Horiuchi, M. Fujiwara, M. Ohba, *Carbon* **2004**, *42*, 2929.
[68] S. Stankovich, D. A. Dikin, R. D. Piner, K. A. Kohlhaas, A. Kleinhammes, Y. Jia, Y. Wu, S. T. Nguyen, R. S. Ruoff, *Carbon* **2007**, *45*, 1558.
[69] Y. Si, E. T. Samulski, *Chem. Mater.* **2008**, *20*, 6792.
[70] Y. Wang, Z. Shi, Y. Huang, Y. Ma, C. Wang, M. Chen, Y. Chen, *J. Phys. Chem. C* **2009**, *113*, 13103.
[71] Y. Chen, X. Zhang, D. Zhang, P. Yu, Y. Ma, *Carbon* **2011**, *49*, 573.
[72] M. J. McAllister, J. L. Li, D. H. Adamson, H. C. Schniepp, A. A. Abdala, J. Liu, M. Herrera-Alonso, D. L. Milius, R. Car, R. K. Prud'homme, I. A. Aksay, *Chem. Mater.* **2007**, *19*, 4396.
[73] H. C. Schniepp, J. L. Li, M. J. McAllister, H. Sai, M. Herrera-Alonso, D. H. Adamson, R. K. Prud'homme, R. Car, D. A. Saville, I. A. Aksay, *J. Phys. Chem. B* **2006**, *110*, 8535.
[74] Z. S. Wu, W. Ren, L. Gao, B. Liu, C. Jiang, H. M. Cheng, *Carbon* **2009**, *47*, 493.
[75] W. Lv, D. M. Tang, Y. B. He, C. H. You, Z. Q. Shi, X. C. Chen, C. M. Chen, P. X. Hou, C. Liu, Q. H. Yang, *ACS Nano* **2009**, *3*, 3730.
[76] Q. Du, M. Zheng, L. Zhang, Y. Wang, J. Chen, L. Xue, W. Dai, G. Ji, J. Cao, *Electrochim. Acta* **2010**, *55*, 3897.
[77] Y. Zhu, M. D. Stoller, W. Cai, A. Velamakanni, R. D. Piner, D. Chen, R. S. Ruoff, *ACS Nano* **2010**, *4*, 1227.
[78] A. Burke, *Electrochim. Acta* **2007**, *53*, 1083.
[79] Z. Lin, Y. Liu, Y. Yao, O. J. Hildreth, Z. Li, K. Moon, C. P. Wong, *J. Phys. Chem. C* **2011**, *115*, 7120.
[80] A. Bagri, R. Grantab, N. V. Medhekar, V. B. Shenoy, *J. Phys. Chem. C* **2010**, *114*, 12053.
[81] J. T. Paci, T. Belytschko, G. C. Schatz, *J. Phys. Chem. C* **2007**, *111*, 18099.
[82] Y. Zhu, S. Murali, M. D. Stoller, A. Velamakanni, R. D. Piner, R. S. Ruoff, *Carbon* **2010**, *48*, 2106.
[83] D. D. L. Chung, *J. Mater. Sci.* **1987**, *22*, 4190.

DOI: 10.1002/smll.201102635

[84] O. Y. Kwon, S. W. Choi, K. W. Park, Y. B. Kwon, *J. Ind. Eng. Chem.* **2003**, *9*, 743.
[85] B. Tryba, A. W. Morawski, M. Inagaki, *Carbon* **2005**, *43*, 2417.
[86] E. H. L. Falcao, R. G. Blair, J. J. Mack, L. M. Viculis, C. W. Kwon, M. Bendikov, R. B. Kaner, B. S. Dunn, F. Wudl, *Carbon* **2007**, *45*, 1367.
[87] Y. Xu, K. Sheng, C. Li, G. Shi, *ACS Nano* **2010**, *4*, 4324.
[88] Z. Sun, T. Hasan, F. Torrisi, D. Popa, G. Privitera, F. Wang, F. Bonaccorso, D. M. Basko, A. C. Ferrari, *ACS Nano* **2010**, *4*, 803.
[89] L. L. Zhang, R. Zhou, X. S. Zhao, *J. Mater. Chem.* **2010**, *20*, 5983.
[90] Q. Wu, Y. Sun, H. Bai, G. Shi, *Phys. Chem. Chem. Phys.* **2011**, *13*, 11193.
[91] L. Zhang, G. Q. Shi, *J. Phys. Chem. C.* **2011**, *115*, 17206.
[92] H. Marsh, R. F. Reinoso, *Activated Carbon*, Elsevier, London **2006**.
[93] V. Barranco, M. A. Lillo-Rodenas, A. Linares-Solano, A. Oya, F. Pico, J. Ibanez, F. Agullo-Rueda, J. M. Amarilla, J. M. Rojo, *J. Phys. Chem. C* **2010**, *114*, 10302.
[94] E. Raymundo-Pinero, P. Azais, T. Cacciaguerra, D. Cazorla-Amoros, A. Linares-Solano, F. Beguin, *Carbon* **2005**, *43*, 786.
[95] T. Liu, T. V. Sreekumar, S. Kumar, R. H. Hauge, R. E. Smalley, *Carbon* **2003**, *41*, 2440.
[96] M. Takeuchi, K. Koike, T. Maruyama, A. Mogami, M. Okamura, *Denki Kagaku* **1998**, *66*, 1311.
[97] M. Takeuchi, T. Maruyama, K. Koike, A. Mogami, T. Oyama, H. Kobayashi, *Electrochemistry* **2001**, *69*, 487.
[98] M. M. Hantel, T. Kaspar, R. Nesper, A. Wokaun, R. Koetz, *Electrochem. Commun.* **2011**, *13*, 90.
[99] Y. Li, M. van Zijll, S. Chiang, N. Pan, *J. Power Sources* **2011**, *196*, 6003.
[100] Y. Zhu, S. Murali, M. D. Stoller, K. J. Ganesh, W. Cai, P. J. Ferreira, A. Pirkle, R. M. Wallace, K. A. Cychosz, M. Thommes, D. Su, E. A. Stach, R. S. Ruoff, *Science* **2011**, *332*, 1537.
[101] Z. Lei, N. Christov, X. S. Zhao, *Energy Environ. Sci.* **2011**, *4*, 1866.
[102] J. Yan, T. Wei, B. Shao, F. Ma, Z. Fan, M. Zhang, C. Zheng, Y. Shang, W. Qian, F. Wei, *Carbon* **2010**, *48*, 1731.
[103] X. An, T. J. Simmons, R. Shah, C. Wolfe, K. M. Lewis, M. Washington, S. K. Nayak, S. Talapatra, S. Kar, *Nano Lett.* **2010**, *10*, 4295.
[104] K. Zhang, L. Mao, L. L. Zhang, H. S. O. Chan, X. S. Zhao, J. Wu, *J. Mater. Chem.* **2011**, *21*, 7302.
[105] E. Yoo, J. Kim, E. Hosono, H. S. Zhou, T. Kudo, I. Honma, *Nano Lett.* **2008**, *8*, 2277.
[106] V. C. Tung, L. M. Chen, M. J. Allen, J. K. Wassei, K. Nelson, R. B. Kaner, Y. Yang, *Nano Lett.* **2009**, *9*, 1949.
[107] G. K. Dimitrakakis, E. Tylianakis, G. E. Froudakis, *Nano Lett.* **2008**, *8*, 3166.
[108] L. Qiu, X. Yang, X. Gou, W. Yang, Z. F. Ma, G. G. Wallace, D. Li, *Chem. Eur. J.* **2010**, *16*, 10653.
[109] D. Yu, L. Dai*J. Phys. Chem. Lett.* **2010**, *1*, 467.
[110] X. Lu, H. Dou, B. Gao, C. Yuan, S. Yang, L. Hao, L. Shen, X. Zhang, *Electrochim. Acta* **2011**, *56*, 5115.
[111] X. Yang, J. Zhu, L. Qiu, D. Li, *Adv. Mater.* **2011**, *23*, 2833.
[112] S. D. Biswas, L. T. Drzal, *ACS Appl. Mater. Sci.* **2010**, *2*, 2293.
[113] S. D. Biswas, L. T. Drzal, *Nano Lett.* **2009**, *9*, 167.
[114] G. Ning, Z. Fan, G. Wang, J. Gao, W. Qian, F. Wei, *Chem. Commun.* **2011**, 5976.
[115] A. Yu, I. Roes, A. Davies, Z. Chen, *Appl. Phys. Lett.* **2010**, *96*, 253105.
[116] L. T. Le, M. H. Ervin, H. Qiu, B. E. Fuchs, W. Y. Lee, *Electrochem. Commun.* **2011**, *13*, 355.
[117] J. J. Yoo, K. Balakrishnan, J. Huang, V. Meunier, B. G. Sumpter, A. Srivastava, M. Conway, A. L. M. Reddy, J. Yu, R. Vajtai, P. M. Ajayan, *Nano Lett.* **2011**, *11*, 1423.
[118] D. W. Wang, F. Li, Z. S. Wu, W. Ren, H. M. Cheng, *Electrochem. Commun.* **2009**, *11*, 1729.
[119] C. T. Hsieh, H. Teng, *Carbon* **2002**, *40*, 667.
[120] K. Kinoshita, *Electrochemical Oxygen Technology*, John Wiley & Sons, New York, **1998**.
[121] C. T. Hsieh, S. M. Hsu, J. Y. Lin, H. Teng, *J. Phys. Chem. C* **2011**, *115*, 12367.
[122] C. Liu, Z. Yu, D. Neff, A. Zhamu, B. Z. Jang, *Nano Lett.* **2010**, *10*, 4863.
[123] T. Y. Kim, H. W. Lee, M. Stoller, D. R. Dreyer, C. W. Bielawski, R. S. Ruoff, K. S. Suh, *ACS Nano* **2011**, *5*, 436.
[124] Y. Cao, T. E. Mallouk, *Chem. Mater.* **2008**, *20*, 5260.
[125] F. Jiang, T. Zhou, S. Tan, Y. Zhu, Y. Liu, D. Yuan, *Int. J. Electrochem. Sci.* **2009**, *4*, 1541.
[126] J. P. Ferraris, M. M. Eissa, I. D. Brotherston, D. C. Loveday, *Chem. Mater.* **1998**, *10*, 3528.
[127] S. Palaniappan, S. L. Devi, *J. Appl. Polym. Sci.* **2008**, *107*, 1887.
[128] K. R. Prasad, N. Munichandraiah, *J. Power Sources* **2002**, *112*, 443.
[129] H. Wang, Q. Hao, X. Yang, L. Lu, X. Wang, *ACS AppL. Mater. Inter.* **2010**, *2*, 821.
[130] C. M. Yang, Y. J. Kim, M. Endo, H. Kanoh, M. Yudasaka, S. Iijima, K. Kaneko, *J. Am. Chem. Soc.* **2007**, *129*, 20.
[131] D. N. Futaba, K. Hata, T. Yamada, T. Hiraoka, Y. Hayamizu, Y. Kakudate, O. Tanaike, H. Hatori, M. Yumura, S. Iijima, *Nat. Mater.* **2006**, *5*, 987.
[132] H. Mi, X. Zhang, S. An, X. Ye, S. Yang, *Electrochem. Commun.* **2007**, *9*, 2859.
[133] E. Frackowiak, V. Khomenko, K. Jurewicz, K. Lota, F. Beguin, *J. Power Sources* **2006**, *153*, 413.
[134] K. Zhang, L. L. Zhang, X. S. Zhao, J. Wu, *Chem. Mater.* **2010**, *22*, 1392.
[135] H. Wang, Q. Hao, X. Yang, L. Lu, X. Wang, *Electrochem. Commun.* **2009**, *11*, 1158.
[136] J. Xu, K. Wang, S. Z. Zu, B. H. Han, Z. Wei, *ACS Nano* **2010**, *4*, 5019.
[137] J. Huang, K. Wang, Z. Wei, *J. Mater. Chem.* **2010**, *20*, 1117.
[138] K. Wang, J. Huang, Z. Wei, *J. Phys. Chem. C* **2010**, *114*, 8062.
[139] H. Wang, Q. Hao, X. Yang, L. Lu, X. Wang, *Nanoscale* **2010**, *2*, 2164.
[140] J. Yan, T. Wei, B. Shao, Z. Fan, W. Qian, M. Zhang, F. Wei, *Carbon* **2010**, *48*, 487.
[141] H. L. Guo, X. F. Wang, Q. Y. Qian, F. B. Wang, X. H. Xia, *ACS Nano* **2009**, *3*, 2653.
[142] X. M. Feng, R. M. Li, Y. W. Ma, R. F. Chen, N. E. Shi, Q. L. Fan, W. Huang, *Adv. Funct. Mater.* **2011**, *21*, 2989.
[143] W. Sugimoto, K. Yokoshima, K. Ohuchi, Y. Murakami, Y. Takasu, *J. Electrochem. Soc.* **2006**, *153*, A255.
[144] V. L. Pushparaj, M. M. Shaijumon, A. Kumar, S. Murugesan, L. Ci, R. Vajtai, R. J. Linhardt, O. Nalamasu, P. M. Ajayan, *Proc. Natl. Acad. Sci. USA* **2007**, *104*, 13574.
[145] K. T. Nam, D. W. Kim, P. J. Yoo, C. Y. Chiang, N. Meethong, P. T. Hammond, Y. M. Chiang, A. M. Belcher, *Science* **2006**, *312*, 885.
[146] D. W. Wang, F. Li, J. Zhao, W. Ren, Z. G. Chen, J. Tan, Z. S. Wu, I. Gentle, G. Q. Lu, H. M. Cheng, *ACS Nano* **2009**, *3*, 1745.
[147] X. Yan, J. Chen, J. Yang, Q. Xue, P. Miele, *ACS Appl. Mater. Inter.* **2010**, *2*, 2521.
[148] T. M. Wu, H. L. Chang, Y. W. Lin, *Compos. Sci. Technol.* **2009**, *69*, 639.
[149] T. M. Wu, S. H. Lin, *J. Polym. Sci. Pol. Chem.* **2006**, *44*, 6449.
[150] S. Bose, N. H. Kim, T. Kuila, K. T. Lau, J. H. Lee, *Nanotechnology* **2011**, *22*, 295202
[151] H. Zhang, G. Cao, W. Wang, K. Yuan, B. Xu, W. Zhang, J. Cheng, Y. Yang, *Electrochim. Acta* **2009**, *54*, 1153.
[152] Y. G. Wang, H. Q. Li, Y. Y. Xia, *Adv. Mater.* **2006**, *18*, 2619.
[153] L. L. Zhang, S. Zhao, X. N. Tian, X. S. Zhao, *Langmuir* **2010**, *26*, 17624.

DOI: 10.1002/smll.201102635

[154] P. A. Mini, A. Balakrishnan, S. V. Nair, K. R. V. Subramanian, *Chem. Commun.* **2011**, *47*, 5753.
[155] S. Chen, J. Zhu, X. Wu, Q. Han, X. Wang, *ACS Nano* **2010**, *4*, 2822.
[156] S. Devaraj, N. Munichandraiah, *J. Phys. Chem. C* **2008**, *112*, 4406.
[157] S. Chen, J. Zhu, X. Wang, *ACS Nano* **2010**, *4*, 6212.
[158] J. Yan, Z. Fan, T. Wei, W. Qian, M. Zhang, F. Wei, *Carbon* **2010**, *48*, 3825.
[159] G. Yu, L. Hu, M. Vosgueritchian, H. Wang, X. Xie, J. R. McDonough, X. Cui, Y. Cui, Z. Bao, *Nano Lett.* **2011**, *11*, 2905.
[160] G. An, P. Yu, M. Xiao, Z. Liu, Z. Miao, K. Ding, L. Mao, *Nanotechnology* **2008**, *19*, 275709.
[161] Z. Fan, J. Chen, M. Wang, K. Cui, H. Zhou, W. Kuang, *Diam. Relat. Mater.* **2006**, *15*, 1478.
[162] X. Xie, L. Gao, *Carbon* **2007**, *45*, 2365.
[163] J. Zhang, J. Jiang, X. S. Zhao, *J. Phys. Chem. C* **2011**, *115*, 6448.
[164] C. C. Hu, Y. T. Wu, K. H. Chang, *Chem. Mater.* **2008**, *20*, 2890.
[165] B. Wang, J. Park, C. Wang, H. Ahn, G. Wang, *Electrochim. Acta* **2010**, *55*, 6812.
[166] J. R. Zhang, D. C. Jiang, B. Chen, J. J. Zhu, L. P. Jiang, H. Q. Fang, *J. Electrochem. Soc.* **2001**, *148*, A1362.
[167] G. Arabale, D. Wagh, M. Kulkarni, I. S. Mulla, S. P. Vernekar, K. Vijayamohanan, A. M. Rao, *Chem. Phys. Lett.* **2003**, *376*, 207.
[168] J. H. Park, O. O. Park, *J. Power Sources* **2002**, *109*, 121.
[169] Z. S. Wu, D. W. Wang, W. Ren, J. Zhao, G. Zhou, F. Li, H. M. Cheng, *Adv. Funct. Mater.* **2010**, *20*, 3595.
[170] H. Li, R. Wang, R. Cao, *Micropor. Mesopor. Mater.* **2008**, *111*, 32.
[171] H. Wang, H. S. Casalongue, Y. Liang, H. Dai, *J. Am. Chem. Soc.* **2010**, *132*, 7472.
[172] X. Du, C. Wang, M. Chen, Y. Jiao, J. Wang, *J. Phys. Chem. C* **2009**, *113*, 2643.
[173] W. Shi, J. Zhu, D. H. Sim, Y. Y. Tay, Z. Lu, X. Zhang, Y. Sharma, M. Srinivasan, H. Zhang, H. H. Hng, Q. Yan, *J. Mater. Chem.* **2011**, *21*, 3422.
[174] Y. C. Zhou, J. A. Switzer, *J. Alloy Compd.* **1996**, *237*, 1.
[175] Y. Wang, C. X. Guo, J. Liu, T. Chen, H. Yang, C. M. Li, *Dalton Trans.* **2011**, *40*, 6388.
[176] S. Chen, J. Zhu, X. Wang, *J. Phys. Chem. C* **2010**, *114*, 11829.
[177] M. J. Deng, F. L. Huang, I. W. Sun, W. T. Tsai, J. K. Chang, *Nanotechnology* **2009**, *20*.
[178] J. Yan, T. Wei, W. Qiao, B. Shao, Q. Zhao, L. Zhang, Z. Fan, *Electrochim. Acta* **2010**, *55*, 6973.
[179] Y. L. Chen, Z. A. Hu, Y. Q. Chang, H. W. Wang, Z. Y. Zhang, Y. Y. Yang, H. Y. Wu, *J. Phys. Chem. C* **2011**, *115*, 2563.
[180] C. Liu, F. Li, L. P. Ma, H. M. Cheng, *Adv. Mater.* **2010**, *22*, E28.
[181] A. Yoshino, *Electrochemistry* **2004**, *72*, 716.
[182] Y. G. Wang, Z. D. Wang, Y. Y. Xia, *Electrochim. Acta* **2005**, *50*, 5641.
[183] Q. T. Qu, Y. Shi, L. L. Li, W. L. Guo, Y. P. Wu, H. P. Zhang, S. Y. Guan, R. Holze, *Electrochem. Commun.* **2009**, *11*, 1325.
[184] X. Hu, Y. Huai, Z. Lin, J. Suo, Z. Deng, *J. Electrochem. Soc.* **2007**, *154*, A1026.
[185] D. W. Wang, H. T. Fang, F. Li, Z. G. Chen, Q. S. Zhong, G. Q. Lu, H. M. Cheng, *Adv. Funct. Mater.* **2008**, *18*, 3787.
[186] Z. S. Wu, W. Ren, D. W. Wang, F. Li, B. Liu, H. M. Cheng, *ACS Nano* **2010**, *4*, 5835.
[187] J. Huang, B. G. Sumpter, V. Meunier, *Angew. Chem. Int. Ed.* **2008**, *47*, 520.
[188] T. Brousse, M. Toupin, R. Dugas, L. Athouel, O. Crosnier, D. Belanger, *J. Electrochem. Soc.* **2006**, *153*, A2171.
[189] T. Cottineau, M. Toupin, T. Delahaye, T. Brousse, D. Belanger, *Appl. Phys. A-Mater.* **2006**, *82*, 599.
[190] D. W. Wang, F. Li, H. M. Cheng, *J. Power Sources* **2008**, *185*, 1563.
[191] N. L. Wu, *Mater. Chem. Phys.* **2002**, *75*, 6.
[192] Q. Cheng, J. Tan, J. Ma, H. Zhang, N. Shinya, L. C. Qin, *Carbon* **2011**, *49*, 2917.
[193] Z. Fan, J. Yan, T. Wei, L. Zhi, G. Ning, T. Li, F. Wei, *Adv. Funct. Mater.* **2011**, *21*, 2366.
[194] J. Yan, T. Wei, W. Qiao, Z. Fan, L. Zhang, T. Li, Q. Zhao, *Electrochem. Commun.* **2010**, *12*, 1279.
[195] H. Wang, Y. Liang, T. Mirfakhrai, Z. Chen, H. S. Casalongue, H. Dai, *Nano Res.* **2011**, *4*, 729.

Received: December 15, 2011
Revised: January 17, 2012
Published online:

DOI: 10.1002/smll.201102635